



UNIVERSIDAD NACIONAL DE COLOMBIA

Reconstructing past fossil fuels CO₂ concentrations using tree rings and radiocarbon in Medellín, Colombia

Marileny Vásquez Piedrahíta

Universidad Nacional de Colombia-Sede Medellín

Facultad de Ciencias Agrarias

Departamento de Ciencias Forestales

Medellín, Colombia

2022



UNIVERSIDAD NACIONAL DE COLOMBIA

Reconstructing past fossil fuels CO₂ concentrations using tree rings and radiocarbon in Medellín, Colombia

Marileny Vásquez Piedrahíta

Thesis presented as partial requirement for the degree of:

Magister en Bosques y Conservación Ambiental

Director:

Jorge Ignacio del Valle Arango

Ms. C. Maestro Universitario, Universidad Nacional de Colombia

Codirector:

Wilson Lara Henao

Postdoctoral Scientist

Universidad Nacional de Colombia-Sede Medellín

Facultad de Ciencias Agrarias

Departamento de Ciencias Forestales

Medellín, Colombia

2022

A mis padres y hermano

Acknowledgements

I thank my parents Dora and Jesús Emilio, my brother, Deiber, and my family in general. I also thank my friends, particularly Jorge Giraldo, Camilo Bedoya, and Liliana Talero, who undoubtedly have helped me immeasurably. Thank especially to the thesis director and Carlos Sierra for all the support and motivation.

I thank the Max Planck Institute for Biogeochemistry in Jena, Germany, to Minciencias, Colombia (project code: 39934), to Wilson Lara for financial support and to the Laboratory of Tropical Dendroecology of the Universidad Nacional de Colombia-Medellín.

Reconstrucción de las concentraciones de CO₂ de combustibles fósiles utilizando anillos de crecimiento y radiocarbono en Medellín, Colombia

Resumen

Para cumplir los compromisos internacionales y nacionales de disminución de las emisiones de combustibles fósiles, las ciudades de todo el mundo deben obtener información sobre sus niveles históricos de emisiones; identificando los puntos calientes que requieren medidas especiales. Las mediciones atmosféricas directas de las fuentes de contaminación son casi imposibles de obtener a posteriori. Sin embargo, los anillos de crecimiento de los árboles constituyen un importante archivo de información medioambiental que puede utilizarse para reconstruir la distribución temporal y espacial de las emisiones y/o concentraciones de combustibles fósiles en las zonas urbanas. Aquí presentamos una metodología novedosa para reconstruir espacial- y temporalmente las concentraciones de CO₂ asociadas con las emisiones de combustibles fósiles [CO₂F] en el área urbana de Medellín, Colombia. Usamos una combinación de análisis dendrocronológicos, mediciones de radiocarbono y modelos estadísticos para obtener mapas anuales de [CO₂F] para el período entre 1977 y 2018. Nuestro método fue exitoso en la identificación de puntos clave alrededor de áreas industriales y de alto tránsito vehicular. También identificó tendencias temporales que pueden estar relacionadas con factores socioeconómicos y tecnológicos. Observamos un aumento importante de [CO₂F] en la última década, y los esfuerzos de las autoridades municipales para reducir el tránsito y las emisiones no parecen tener un efecto significativo en la contribución de los combustibles fósiles al aire local. El método que aquí se presenta podría ser de gran valor para que los planificadores de las ciudades y los funcionarios de medio ambiente identifiquen los puntos claves de las emisiones, evalúen el impacto de las políticas medioambientales y planifiquen nuevas estrategias para reducir las emisiones y cumplir los compromisos de disminución de las emisiones de combustibles fósiles.

Palabras clave: dendrocronología, radiocarbono, emisiones de combustibles fósiles, CO₂ fósil

Abstract

To meet international and national commitments to decrease emissions of fossil fuels, cities around the world must obtain information on their historical levels of emissions, identifying hotspots that require special attention. Direct atmospheric measurements of pollution sources are almost impossible to obtain retrospectively. However, tree rings serve as an archive of environmental information for reconstructing the temporal and spatial distribution of fossil fuel emissions in urban areas. Here, we present a novel methodology to reconstruct the spatial and temporal contribution of fossil fuels' CO₂ concentration ([CO₂F]) in the urban area of Medellin, Colombia. We used a combination of dendrochronological analysis, radiocarbon measurements, and statistical modeling. We obtained annual maps of [CO₂F] from 1977 to 2018 that describe changes in their spatial distribution over time. Our method was successful in identifying hotspots of emissions around industrial areas, and areas with high traffic density. It also identified temporal trends that may be related to socioeconomic and technological factors. We observed an important increase in [CO₂F] during the last decade, which suggests that efforts of city officials to reduce traffic and emissions did not have a significant impact on the contribution of fossil fuels to local air. The method presented here could be of significant value for city planners and environmental's officials from other urban areas around the world. It allows identifying hotspots of fossil fuel emissions, evaluating the impact of previous environmental policies, and planning new interventions to reduce emissions and meet commitments to decrease fossil fuel emissions.

Keywords: dendrochronology, radiocarbon, fossil fuels emissions, fossil CO₂

Contents

	Pág.
Content	
1. Theoretical framework	13
1.1 Detection of fossil fuel pollution using annual tree rings.....	13
1.2 Annual tree rings in tropical trees.....	17
2. Introduction	20
3. Materials and methods	22
3.1 Study area.....	22
3.2 Dendrochronological analysis	22
3.2.1 Sampling.....	22
3.2.2 Crossdating.....	23
3.3 Radiocarbon analysis	24
3.3.1 Determination of radiocarbon	24
3.3.2 Calculation of the CO ₂ concentration of fossil fuels origin [CO ₂ F].....	26
3.3.3 Comparison with official reports on CO ₂ emissions.....	29
3.3.4 Time interpolation.....	29
3.3.5 Spatial analysis	30
4. Results	31
4.1 Dendrochronological analysis	31
4.2 Temporal patterns in radiocarbon and [CO ₂ F]	31
4.3 Comparison with emission data	33
4.4 Time-series analysis	35
4.5 Spatial analysis.....	38
5. Discussion	41
6. Conclusions	46
7. Appendix A: Residual chronology	47

8. Appendix B: Tree ring descriptions.....	48
9. Appendix C: Radiocarbon values	49
10. References	59

List of figures

- Figure 1:** Radiocarbon concentration in the background air and in the measured tree rings expressed as $\Delta^{14}\text{C}$ (‰) over time. The red dots indicate the annual concentrations measured in the tree rings of *Fraxinus udhei* from the urban area of Medellín (UAM). The black line represents the background “clean air” concentration obtained from the North Hemisphere Zone 3 (NH3) curve. 32
- Figure 2:** The concentration of fossil fuels CO_2 [COF] values over time in ppm for the urban area of Medellín between 1977 and 2018. The vertical bars indicate the standard deviation between tree rings. Numbers above the bars indicate the sample size for ^{14}C analysis. 33
- Figure 3:** Comparison between average values of the concentrations of fossil fuels calculated in this study and official CO_2 emission data for the urban area of Medellín reported in official reports during the years 2000-2018. In this regression $p < 2.5 \times 10^{-5}$, $R^2 = 0.66$ 34
- Figure 4:** Mixed-effects model of the concentrations of fossil fuels CO_2 [CO2F] over time. Each number indicates the tree code. The dots represent the calculated [CO2F] data based on the ^{14}C analyses made to each tree, and the lines represent predictions from the fixed-effect model. 36
- Figure 5:** Spatial interpolation of fossil fuels concentrations [CO2F] (scale bar in ppm) across the urban area of Medellín, in five-year windows between 1980-2015 and for the year 2018. Red dots in each window represent the location of the 35 trees of *F. uhdei*. On the right side is the urban area of Medellín city for the year 2020. The red dots are the 35 trees of *F. uhdei* with their respective code. 39
- Figure 6:** Uncertainty map of spatial interpolations of fossil fuel concentrations [CO2F] (scale bar in ppm) across the urban area of Medellín, between 1980-2018; the white dots represent the location of the 35 trees of *F. uhdei*. 40

List of tables

	Pág.
<i>Table 1: Parameter estimators of the mixed-effects model for the fossil-fuel CO₂ concentrations over time. The variables time and [CO₂F] represent the fixed effects, and the trees the random effects.</i>	37
<i>Table 2: ANOVA to compare the mixed-effects model (M1) and an equivalent model with no random effects (M0).....</i>	37

1. Theoretical framework

1.1 Detection of fossil fuel pollution using annual tree rings

Some techniques used to assess contamination are ice cores, peat cores, and annual laminated sediments-varves- (Bancone *et al* 2020, Beaudon *et al* 2017, Dong *et al* 2021, Machado *et al* 2008, Berg *et al* 2008). However, they are generally expensive, and their geographical distribution is uneven. To this end, bioindicators are an alternative because of their even spatial distribution and low cost.

With bioindicators, the responses of organisms to changes in the environment are measured, basically referring to the accumulation of pollutants that depend on the species and its sensitivity (Michel Herrera 2016). Mosses, lichens, plankton, animals, herbs, annual plants, shrubs, and trees, among others, have been used as bioindicators for monitoring pollution (Figueira *et al* 2002, Varga *et al* 2020, Scerbo *et al* 1999, Parmar *et al* 2016, Sawidis *et al* 2011). In the case of trees, various components - leaves, roots, fruits, bark, or wood - have acted as indicators of contamination (Karmakar *et al* 2021, Terekhina and Ufimtseva 2020, Varga *et al* 2020, Burken *et al* 2011, Madejo *et al* 2006).

Dendrochronology studies events through time recorded in the tree-ring structures or dated by annual tree rings (Binda *et al* 2021, Speer 2010, Kaennel and Schweingruber 1995). These events are recorded in the tree rings in both physical and chemical signals. Physicals signals, such as the width of the rings, maximum density, hydraulic structure, and scars in the rings, among others (Binda *et al* 2021, Aguilera-Betti *et al* 2020, Guibal and Guiot 2020, Speer 2010). Chemicals signals, such as the isotopes content of ^{14}C , ^{12}C , ^{13}C , ^{18}O , ^{16}O , the N and S content, and the heavy metals (Loader *et al* 2019, Cesur *et al* 2021, D'Arcy *et al* 2019, Shestakova and Martínez-Sancho 2021). The subdisciplines of dendrochronology arise when growth rings are used in the study of phenomena that are part of other sciences: dendroclimatology,

dendrohydrology, dendroecology, dendroarchaeology, dendrogeomorphology, dendropyrochronology, dendrovolcanology, dendroentomology, dendroglaciology, and dendrochemistry among others (Aguilera-Betti *et al* 2020, Speer 2010, Kaennel and Schweingruber 1995). The detection and dating of the chemical signals constitute the sub-discipline of dendrochemistry (Speer 2010, Kaennel and Schweingruber 1995, Shestakova and Martínez-Sancho 2021). For this reason, trees with annual rings are considered living stations for monitoring, retrospectively, the atmosphere quality (Binda *et al* 2021, Balouet *et al* 2007, Burken *et al* 2011, Cutter and Guyette 1993, Krepkowski *et al* 2011, Semeraro *et al* 2020). In this context, the chemical analysis of tree rings can be used as a proxy to read historical changes in the atmosphere environment (Binda *et al* 2021, Hou *et al* 2020, Djuricin *et al* 2012) (see introduction chapter).

There are three isotopes of carbon in the atmosphere CO₂: ¹²C (99%), ¹³C (1%), and ¹⁴C (1x10⁻¹²%) (Graven *et al* 2020). Through photosynthesis, trees capture atmospheric CO₂ that is fixed in the form of cellulose (Alberte *et al* 1976, Binda *et al* 2021, Dongarrà and Varrica 2002, Shestakova and Martínez-Sancho 2021). During the chemical and enzymatic reactions of photosynthetic activity, plants discriminate the ¹³C isotope in favor of ¹²C, although this discrimination is less in dry periods when there are limitations in the water supply (Busch *et al* 2020, Rozendaal and Zuidema 2011, Binda *et al* 2021). Plants do not discriminate against ¹⁴C, the only unstable and radioactive isotope, which also originates from the impact of galactic cosmic rays with ¹⁴N in the atmosphere. ¹⁴C has a half-life of 5,568 years ± 30 years (Kutschera 2019, Bowman 1990); that is, every 5,568 years, 50% of the ¹⁴C in organic matter is transformed into ¹⁴N (Kutschera 2019). Since fossil fuel has an age of over three hundred million years, it does not have ¹⁴C (Pataki *et al* 2010, Rakowski *et al* 2008a).

Given that trees in the process of photosynthesis fix the three isotopes of C, it can be considered that their concentrations in the wood may be analogous to the isotopic composition of the atmosphere at the time of fixation (Dongarrà and Varrica 2002, Pataki *et al* 2010, Sensuła and Pazdur 2013).

One application of dendrochemistry is to perform a retrospective analysis of the atmospheric concentration of CO₂ from fossil fuel in growth rings in urban or industrial areas, considering

the non-existence of ^{14}C in fossil fuels. Therefore, ^{14}C in the tree rings is a marker of pollution from fossil fuel burning (Beramendi-Orosco *et al* 2017, Kontul' *et al* 2017, Flores *et al* 2017, Jeřkovský *et al* 2015).

A metric of pollution of the atmosphere with fossil fuel is the difference, year by year, between the ^{14}C concentration on-air of a non-polluted fossil fuel site and the ^{14}C in tree rings of an urban or industrial area. This phenomenon is known as the dilution effect or Suess effect of atmospheric ^{14}C in polluted areas (Suess 1955).

Another option to detect the Suess effect is to measure the ^{14}C on air at monitoring stations in cities or industrial areas and compare it, year by year, with ^{14}C of the closest data measured at "clean air" stations that have recorded this information during the last 50 to 67 years in various Earth's sites. This option is much more expensive to the point that it only exists for a few First World cities (Varga *et al* 2020, Miller *et al* 2020, Zhao *et al* 2021).

The ^{14}C from annual tree rings is such a good proxy for the annual mean ^{14}C measured directly from the air that the curve called Northern Hemisphere 3 (NH3), used for ^{14}C calibration purposes, and which includes our study area, is a compilation of atmospheric radiocarbon from 1950 to 2019 derived from both atmospheric CO_2 sampling and tree rings from "clean-air" sites (Hua *et al* 2021).

Fossil-fuel pollution monitoring stations allow the concentration of $^{14}\text{CO}_2$ to be determined sub-annually-hours, days, weeks, months- (Vogel *et al* 2010). With tree rings, such fine measurements cannot be achieved. However, virtually no city has enough direct measurement stations to temporarily and spatially study fossil fuel pollution. The tree rings, proxies of these stations, allow these studies (Djuricin *et al* 2012, Hou *et al* 2020, Sensuła *et al* 2018). Perhaps the only practical way to know, retrospectively, the behavior of pollution by fossil fuel before the direct measurement is through the tree rings. To study the Suess effect, most researchers have used the approach proposed by (Levin *et al* 2003, Levin 1987) for the mass balance equations.

The concentration of the CO_2 fossil in the tree rings sampled $C_m = [\text{CO}_2F]$ consists of three concentrations components, a background component C_b , a biosphere component C_{bio} , and a fossil fuel component C_f (Levin *et al* 2003). So, the first mass balance equation (1) is:

$$C_m = C_b + C_f + C_{bio}, \quad (1)$$

The $\Delta^{14}C$ of these components are, respectively, $\Delta^{14}C_m$, $\Delta^{14}C_b$, $\Delta^{14}C_{bio}$. See equation (6). The second mass balance equation (2) is:

$$\begin{aligned} C_m(\Delta^{14}C_m + 1000\text{‰}) &= C_b(\Delta^{14}C_b + 1000\text{‰}) + \\ &C_f(\Delta^{14}C_f + 1000\text{‰}) + C_{bio}(\Delta^{14}C_{bio} + 1000\text{‰}), \end{aligned} \quad (2)$$

The second term to the right of equation (2) is zero since $\Delta^{14}C_f = -1000\text{‰}$. And $\Delta^{14}C_{bio} = \Delta^{14}C_f$ as the major flux from the biosphere comes from autotrophic respiration, a young reservoir in very close ¹⁴C equilibrium with atmospheric CO₂. Combining both equations leads to equation (6) in methods, first derived by (Levin *et al* 1989). Then equation (1) becomes equation (7). Also, note the derivation in equations (10) through (12).

In equation (2), some authors do not match but do a record that $\Delta^{14}C_{bio} \approx \Delta^{14}C_b$ (Vogel *et al* 2010, Djuricin *et al* 2012). Because there is no $\Delta^{14}C_{bio}$ data available, and the low marginal effect of this component in the results of [CO₂F], it is omitted (Palstra *et al* 2008, Zhou *et al* 2014, Hou *et al* 2020, Turnbull *et al* 2014).

As fossil fuel has not ¹⁴C, we used -1000‰ to represent the radiocarbon signature of $\Delta_m^{14}C$. But modern additives and bioethanol in gasoline slightly enrich $\Delta^{14}C_m$. For $\Delta^{14}C_m$ (Djuricin *et al* 2010), found in Irvine, California $-954 \pm 4\text{‰}$, and (Affek *et al* 2007) in Pasadena, California reported -960‰ . However, the mass balance model is not sensitive to minor deviations in the constituents' signatures due to very large differences in their absolute values (Djuricin *et al* 2010, 2012) the studies that we have consulted assume $\Delta^{14}C_m = -1000\text{‰}$ (Pazdur *et al* 2007, Battipaglia *et al* 2010, Beramendi-Orosco *et al* 2015, 2017, Cain 1978, Capano *et al* 2010, Flores *et al* 2017, Jeřkovský *et al* 2015, Kontul' *et al* 2017, Beramendi-Orosco *et al* 2013a, Xu *et al* 2016, Rakowski *et al* 2013a, 2008b, 2004a, 2004b, 2001, Piotrowska *et al*

2019, Hou *et al* 2020, Sensuła *et al* 2018). If in densely populated cities and where the use of additives is massive, the tiny error induced by this assumption is negligible, in less populated and lesser use of additives, this error should be even smaller.

1.2 Annual tree rings in tropical trees

The Greek philosopher Theophrastus, the botanist, is credited with the first discovery of annual rings in 322 BC ¹(Speer 2010, Sarton 1954). But, the Theophrastus statement (Studhalter 1956) was, "... and if one forces a stone or some similar object into a tree, it becomes hidden, since the new growth surrounds it, as was the case with the wild olive tree which stood in the marketplace at Megara". So, Theophrastus doesn't say anything about annual tree rings. Between 1452 and 1519, Leonardo da Vinci wrote in the *Trattato della pittura:* " *Li circuli delli rami degli alberi segati mostrano il numero delli suoi anni, eguali furano piú umidi, o piú secchi la Maggiore o minore loro grossezza.*" The circles of the branches of the sawn trees show the number of their years, and that they were wetter, or drier, the greater or lesser their thickness. This is a basic principle in dendroclimatology² (Speer 2010, Studhalter 1956, Sarton 1954). In a diary from 1581, French philosopher Michel de Montaigne wrote that an Italian carpenter told him that trees form a ring each year (Sarton 1954).

In the experiments of the French forester Duhamel du Monceau in 1751 and 1757 of marking the bark and wood of trees, he was able to delimit the radial growth of a single season, thereby dating a growth ring accurately. As long ago as 1787, the German forester Burgsdorf used an ax mark made in 1767 on an oak tree at a boundary line as proof that only one ring is formed in a year. In 1785, over the scar line had been 18 rings. The significance of the woody overgrowth covering dates, initials, and other markings cut through the bark is discussed by many writers beginning with Bartolinus 1654 (Speer 2010, Studhalter 1956).

¹ <http://www.inkstain.net/fleck/2004/01/leonardo-and-the-tree-rings/>

² <https://hmong.es/wiki/Dendrochronology>

The crossdating or synchronization of the-rings width is the most relevant feature of dendrochronology as a scientific discipline. The Frenchmen Duhamel du Monceau and Lois Leclerc conde de Buffon in 1737, counted back to the wood ring of 1708 -1709, one of the coldest years in Europe, in which they found a severe frost injury. Years later, independently, Linnaeus (1745, 1751) in Sweden and Ludwig von Burgsdorf (1783) in Germany again had counted back to the same winter. If these data are combined into one, we have here the beginning of crossdating because the growth ring of 1708 -09 was identified in several trees.

Johan Leche, a naturalist, and Professor of Medicine in Finland, instead of winter harshness, studied the dry and hot summer of 1757 that killed and damaged several trees and tree species. Whereas in Leche's three writings of 1757 and 1763, he used several trees (Norrgård and Helama 2021), he should be considered the first scientist to carry out a crossfading.

During the 19th and early 20th centuries, crossdating was developed by numerous scientists, among them, the astronomer A. E. Douglass (Douglass 1909, Webb 1983), called the father of dendrochronology (Speer 2010), who invented the skeleton plot technique in 1941 (Douglass 1941), still in use.

Some evidence shows that 18th and early 19th century Central European foresters used tree rings to study the growth (in diameter, volume) of trees and forests depending on age. They extended their growth curves to ages over more than 200 years. For example, the growth curves of Georg Ludwig Hartig (Hartig 1795) among many other cited by (Romberger and Mikola 1964) and (Prodan 1968) reproduced in Prodan's (1968, p. 342-344) book. These studies can only be done with dendrochronology using annual tree rings. Permanent sampling plots in forests measured for more than 200 years have never existed. Theodor Hartig (Hartig 1853) published, as far as known, the first literature review on growth rings of perennial plants in Germany.

Sir Dietrich Brandis was a botanist and forester from Germany who worked with the British Imperial Forestry Service in colonial India for nearly 30 years (1856-1883) coming to be Inspector

General of Forests in India from 1864 to 1883. Brandis is considered the father of tropical forestry. During the nineteenth century, foresters in continental Europe had no prejudices about the non-existence of annual rings in tropical trees (Worbes 2002). For this reason, since his arrival in India, Brandis studied the growth of teak (*Tectona grandis*) and of other tree species using tree rings under the correct assumption that they were annuals (Brandis 1960, 1979, Deepak *et al* 2010). The first formal demonstration of the existence of annual rings in a tropical species comes from (Geiger 1915) in *T. grandis*. The astronomer (Berlage 1931) developed a chronology of 415 years with the rings of teak (*T. grandis*) in Java. In addition to crossdating, he was perhaps the first scientist to standardize the width of the tree rings time series.

(Coster 1923, 1926, 1927) carried out several phenological and physiological experiments on Indonesian trees. In addition to his discovery of hormones, he has found numerous species with annual rings. With the exception of Brandis' research, pioneering dendrochronological studies in the tropics were written in German and Dutch. Perhaps for this reason they were little known.

The first article on annual rings in the African tropics was by (Hummel 1946) and in the American tropics (Hastenrath 1963). Except for tropical ever-wet forests, annual tree rings exist in all tropical environments where trees grow: mangroves, wooded savannahs, high mountains up to about 5000 masl, floodplain forests, and tropical dry and rain forests (Aguilera-Betti *et al* 2020, Brienen *et al* 2016, Schöngart *et al* 2017). The last frontier, the tropical ever-wet forests, was recently crossed in the Chocó region, the rainiest forest of the Americas, Colombia (Giraldo 2021).

2. Introduction

Annual tree rings are both powerful paleoclimatic tools and bio-indicators. They can be used to spatially reconstruct historical levels of chemical properties of air, such as the concentration of heavy metals, radioactive elements, and other polluting compounds. Pollutants enter trees through stomata, bark, and roots, eventually accumulating in tree rings (Balouet *et al* 2007, Burken *et al* 2011). Through photosynthesis, trees fix ¹²C (98.89%), ¹³C (1.11%), and ¹⁴C (10⁻¹⁰%) from atmospheric CO₂ and use this carbon to produce tree-ring wood. During a particular year, ¹⁴C used to produce tree-ring wood can be considered analogous to the ¹⁴CO₂ in the atmosphere at the time of fixation (Dongarrà and Varrica 2002, Pataki *et al* 2010, Worbes 1999, Sensuła and Pazdur 2013). Therefore, ¹⁴C can be used as an isotopic marker of CO₂ from fossil fuels origin. The burning of fossil fuels is the foremost source of increased atmospheric CO₂ during previous decades (Grubler *et al* 2012). Fossil fuels are devoid of ¹⁴C; for this reason, their emissions reduce the ¹⁴CO₂ to ¹²CO₂ ratio, allowing one to obtain estimates of the contribution of fossil fuels burning to local air. Thus, the difference in the isotopic concentration of air from a clean area versus air from urban or industrial areas can be used to calculate the percentage contribution of CO₂ derived from fossil fuels (Djuricin *et al* 2012, Turnbull *et al* 2016). This phenomenon is known as the Suess effect (Suess 1955) or dilution effect of atmospheric ¹⁴C in polluted areas (Levin *et al* 1989). While in urban areas the uncertainty from direct measurements of the Suess effect is higher due to the high degree of spatial and temporal variability of CO₂ (Wang *et al* 2021), and several years of measurement are required, tree rings are an alternative to document this perturbation to direct atmospheric measurements.

Previous studies have demonstrated the utility of tree ring analysis and ¹⁴C measurements to temporally reconstruct fossil fuels emissions in different cities around the world (Battipaglia *et al* 2010, Cain 1978, Rakowski *et al* 2004a, 2004b, 2008a, 2013a, 2013b, Pazdur *et al* 2007, Capano *et al* 2010, Rakowski *et al* 2001, Xu *et al* 2015, 2016, Ješkovský *et al* 2015, Flores *et al* 2017, Kontul' *et al* 2017, Beramendi-Orosco *et al* 2015, 2013a, 2017). Other studies have shown that

this method is also useful for spatial reconstructions (Piotrowska *et al* 2019), or both temporal and spatial (Djuricin *et al* 2012, Sensuła *et al* 2018, Hou *et al* 2020). All studies have found that the higher ^{14}C values correspond to cleaner habitats from remote high elevation areas. In contrast, low values are associated with fossil fuels emissions in densely populated areas with larger industrial and traffic footprints, corresponding to more polluted atmospheres. However, probably due to the high cost of radiocarbon analysis, most studies only provide a snapshot of the contribution of fossil fuels in urban environments. More comprehensive spatial and temporal reconstructions spanning several decades, and different city environments still have to be done to demonstrate the high potential of this method for the design or evaluation of policies aiming at reducing emissions of fossil fuels.

One advantage of tree rings, compared to other studies based on the direct atmospheric sampling of $^{14}\text{CO}_2$, is that trees can be sampled multiple times over a large spatial domain. Therefore, the history of emissions in urban environments can be reconstructed in space and time, which can be of immense value for cities planners and policymakers. With these considerations in mind, we designed a study to address the question: Can we reconstruct, in time and space, the fossil fuels CO_2 concentrations [CO2F] in the urban area of Medellín, Colombia, using dendrochronological and isotopic methods? Therefore, our objectives were to (i) develop a statistical model to reconstruct [CO2F] in space and time using dendrochronology and radiocarbon methods, (ii) characterize the changes in [CO2F] that have occurred spatially and temporally in a large urban area with significant population growth, and (iii) discuss possible factors that have induced changes in [CO2F] in space and time. Our a priori expectations were that the spatial and temporal reconstruction method identifies different zones, such as residential, with a low vehicular flow, and industrial, with high contributions of emissions that dilute the local $^{14}\text{CO}_2$ air. To our knowledge, this is the first time that such comprehensive analysis has been done on an urban area using tree rings.

3. Materials and methods

3.1 Study area

This study was conducted in the urban area of Medellín (UAM), Colombia, a South American city located in the North of the Andes Mountain Range, from 6°17'40" to 6°11'58"N, and 75°17'40" to 75°32'56"W. The mean annual temperature is 21.6 ° C, the mean annual precipitation is 1612 mm, January is the driest month with 52 mm on average, and October is the wettest, with 207 mm on average. The mean altitude is 1475 m. The city is part of the Aburrá Valley Metropolitan Area. The city's inhabitants are currently above 2.5 million and have increased in previous decades due to massive immigration from other parts of Colombia and Venezuela.

3.2 Dendrochronological analysis

3.2.1 Sampling

Thirty-five urban trees of *Fraxinus uhdei* (Wenz.) Lingelsh located across the UAM, were sampled using an increment borer by taking three cores from each tree. We have selected this species because previous studies demonstrated it forms annual rings in tropical environments (Miranda-Áviles *et al* 2009, Villanueva Díaz *et al* 2015) ; furthermore. Also, it is a widely and evenly planted species at UAM since the mid-1950s. We selected visually healthy trees located along major streets, excluding trees with evidence of excessive pruning or symptoms of diseases or plagues. The core samples were mounted on prefabricated wooden supports, dried for 12 hours at 35°C, and sanded with increasing grit number sandpaper (60–1200) to improve visualization of wood anatomy. Each core was scanned at 1800 dpi using an Epson Expression 10000XL scanner,

calibrated by Regent Instruments from Canada for dendrochronological studies. Tree rings were marked within 0.014 mm accuracy using the *ImageJ* program (Schneider *et al* 2012). Tree-ring widths (TRWs) were measured on the scanned images using a script programmed using the R statistical environment (R Core Team 2020). The script processes points in the scanned images selected with the selection tools of *ImageJ* and computes the Euclidean distance between selected points.

3.2.2 Crossdating

The quality of the dates assigned to the TRWs was controlled by crossdating (Speer 2010). This technique allowed us to identify the exact year in which each tree ring was formed and served as statistical control for the visual identification of the TRWs. The crossdating consisted of comparing the TRWs series within the same tree and between different trees using different parametric indicators (Speer 2010). Crossdating was carried out with the R package *dpLR* (Dendrochronology Program Library) (Bunn 2008). The crossdating was carried out with the R package *dpLR* (Dendrochronology Program Library) (Bunn 2008). Signal-to-noise ratio (SNR), expressed population signal (EPS), and mean sensitivity (MS) were calculated following Cook and Kairiukstis (1990), as shown below.

$$SNR = \frac{N\bar{r}}{(1 - \bar{r})}, \quad (3)$$

where N is the number of trees, and \bar{r} defined as the mean series inter correlation calculated between all possible pairs of indexed series drawn from different trees.

$$EPS = \frac{N\bar{r}}{N\bar{r} + (1 - \bar{r})}, \quad (4)$$

$$MS = \frac{1}{n-1} \sum_{t=1}^{t=n-1} \left(\frac{2(X_{t+1} - X_t)}{X_{t+1} + X_t} \right), \quad (5)$$

where X_t is ring width in year t , X_{t+1} is ring width in the following year, and n is the number of years being compared.

3.3 Radiocarbon analysis

3.3.1 Determination of radiocarbon

We extracted the α -cellulose from a complete core from each sampled tree. Then, by comparing the core after α -cellulose extraction with the other core replicates of the same tree, we extracted α -cellulose samples for ¹⁴C analysis of one out of every four rings and assigned the corresponding calendar year. From each ring, we extracted about 30 mg from latewood α -cellulose. Although, it is stated that alpha-cellulose comes from tree-ring formation's year. It is also well established that non-structural carbon (NSC) constituted by sugars and starch from previous years migrates towards the forming growth ring. Thus, the age of the NSC is less than that of the growth ring (Trumbore *et al* 2015, Santos *et al* 2020). To reduce possible contamination with NSC, we avoid extracting wood for ¹⁴C analysis from the earlywood of the tree rings. A total of 282 ¹⁴C samples

were analyzed, which, on average, are equivalent to eight rings per tree. We extracted the α -cellulose in a Soxhlet system at the Laboratory of Agro-industrial Processes of the Universidad Pontificia Bolivariana in Medellín. This laboratory followed the protocol established by Durgante (2017) to control biases in the radiocarbon analysis due to contamination of the sampled cellulose. To obtain α -cellulose, the wood is subjected to two extraction processes as follows:

a. Lipid extraction:

- To place the samples in the Soxhlet.
- Prepare the 600 ml solution of toluene and ethanol 2:1 and place in the soxhlet.
- Build the Soxhlet system and turn on at a temperature of 6.5-7°C. Let it run for 24 hours.
- Remove the samples and allow them to dry for 2 hours.
- Repeat extraction with 600 ml ethanol for 24 hours.
- Dry the samples for 2 hours

b. Bleaching:

- Place the samples in the Becker
- Add 600 ml of deionized water and let the samples boil for 2 hours.
- Mix the 600 ml solution of deionized water and place the stirrer in the Becker to start the solution-
- Wait for the water to reach 70°C.
- Measure 4 g of sodium chlorite and 2 ml of acetic acid.
- Add the acetic acid and sodium chlorite to the water at the same time.
- Change the solution every 3-4 hours. This can be done every 3 to 4 days
- Add more sodium chlorite and more acetic acid. Control the temperature (about 70°C).
- When the tissue samples are white, place them in 600 ml of deionized water and rinse them several times over a period of 3 to 4 hours.

After the α -cellulose was extracted, the samples were transformed to graphite and then the radiocarbon concentration was measured using accelerator mass spectrometry (AMS) at the Max Planck Institute for Biogeochemistry in Jena, Germany (Steinhof *et al* 2017).

3.3.2 Calculation of the CO₂ concentration of fossil fuels origin [CO₂F]

Concentrations of fossil fuels [CO₂F] (ppm) were estimated by processing the radiocarbon concentration data and combining two mass balance equations (Levin *et al* 1989, 2003) we obtain the following formula

$$[CO_2F] = C_b \left(\frac{\Delta_b - \Delta_m}{\Delta_m + 1000} \right), \quad (6)$$

where [CO₂F] is the estimated mole fraction, in ppm, of CO₂ derived from fossil emissions sources, C_b is the atmospheric CO₂ mole fraction in the background area, Δ_b and Δ_m are the ¹⁴C isotope ratios (in ‰) for the background air and for the measured sample at the UAM, respectively. As the C_b has not been measured in the background area, we assumed it corresponds to the annual mean values reported for the Mauna Loa station in Hawái, considering it represents the global clean air (Tans and Kirk 2018). For the Δ_b , we used $\Delta^{14}C$ data from the Northern Hemisphere Zone 3 curve (Hua *et al* 2021), corresponding to the time-span from 1977 to 2018.

Although the equation to compute the contribution of fossil fuels CO₂ ([CO₂F]) to local air is relatively well known (Levin *et al* 2003, Turnbull *et al* 2016), we found some inconsistencies in the tree-ring literature, and therefore we provide here our own mathematical derivation. We hope this derivation helps to disambiguate previous inconsistencies and can be used in the future better to determine what equation to use in computing [CO₂F].

For simplicity of mathematical notation, we use in this derivation c_f , instead of [CO₂F], but they are the same quantity. The concentration of atmospheric CO₂ measured at any given point

(c_m) can be expressed as the sum of two concentrations: background air (c_b) and fossil fuels (c_f)³ so

$$C_m = C_b + C_f, \quad (7)$$

Following (Levin *et al* 2003) the equivalent isotopic composition equation can be expressed as

$$\Delta_m C_m = \Delta_b C_b + \Delta_f C_f, \quad (8)$$

where $\Delta = \Delta^{14}\text{C} + 1000 \text{ ‰}$. If fossil fuels have a $\Delta^{14}\text{C} = -1000 \text{ ‰}$, then $\Delta_f = 0$ and equation (8) can be expressed as

$$C_m = \frac{\Delta_b C_b}{\Delta_m}, \quad (9)$$

Replacing equation (9) into equation (7), we have

$$C_f = C_b \frac{\Delta_b - \Delta_m}{\Delta_m}, \quad (10)$$

Alternatively, equation (8) can be expressed as

$$C_b = \frac{\Delta_m C_m}{\Delta_b} \quad (11)$$

and replacing this expression into equation (7), we obtain an alternative expression for c_f

$$C_f = C_m \frac{\Delta_b - \Delta_m}{\Delta_b}, \quad (12)$$

One can use either equation (10) or (12) to compute c_f . Equation (12) is useful only if the CO₂ concentration was measured at the point of interest. However, equation (10) is more useful when this concentration is not known, but the background CO₂ concentration is known (e.g., from the Mauna Loa observatory). This is our case.

The equations we obtained here (eq. 10 and 12) are different than reported by other authors in the tree-ring radiocarbon literature (Rakowski *et al* 2008a, Beramendi-Orosco *et al* 2017). We were not able to mathematically derive the equation for [CO₂F] reported by these authors, which, in our notation above, would be expressed as:

$$c_f = c_b \frac{\Delta_b - \Delta_m}{\Delta_b} \quad (13)$$

In our calculations, the use of this equation leads to very small deviations from the equation used in our manuscript (eq. 10). This implies that although the equation used in previous studies is likely wrong, it does not provide results that are substantially different than would be obtained using the correct equation. Nevertheless, we believe that, for future studies, it is important to use the mathematically correct equation (eqs. 10 or 12).

3.3.3 Comparison with official reports on CO₂ emissions

The [CO₂F] values, in ppm, were compared with official UAM CO₂ emission records (in Tg C yr⁻¹) (Toro *et al* 2013, 2015, 2017, 2018). [CO₂F] values were averaged, according to the temporal resolution of the CO₂ emissions records obtained (2000-2018). We fitted an exponential regression model between [CO₂F] and the records of CO₂ emissions to evaluate the degree of agreement between the [CO₂F] concentration values and the total emission values. The parameter estimates compared were the probability of the *F*-statistic, the coefficient of determination, and the significance level (99%).

3.3.4 Time interpolation

Since [CO₂F] was calculated from radiocarbon analysis at discontinuous time steps, [CO₂F] values for the years studied were estimated using a mixed-effects model that predicts [CO₂F] as a function of time and quantifies random effects on the model parameters. Preliminary analysis of the scatter plots of [CO₂F] over time indicated polynomial patterns in all trees with deviations in residual variance due to core variability. Therefore, in the mixed model, the effect of each core on the polynomial trend of the series was as follows.

$$[CO_2F]_{s,t} = a_{0s} + a_{1s} \cdot t_s + a_{2s} \cdot t_s^2 + e_{s,t};$$

$$e_{s,t} \sim N(0, R_s),$$
(14)

where numeric subscripts indicate fixed effects, alphabetic subscripts (*s*) indicate random effects at tree level, *t* is time (yr); *e_{s,t}* is a vector of normalized residuals, *R_s* is the variance-covariance

matrix of the residuals. The variables, time (t) and [CO₂F], were fitted as fixed effects and the tree as random effects. Improvements in the model by accounting for tree variability were measured using Akaike's Information Criterion (AIC) and maximum likelihood ratio-tests between the mixed-effects model and an equivalent equation without random effects (Pinheiro and Bates 2000). This mixed-effects model was fitted with the nlme (Linear and Nonlinear Mixed-Effects Models) package (Pinheiro *et al* 2021) of the R software.

3.3.5 Spatial analysis

Here we assume that the spatial distribution of [CO₂F] across the UAM is mainly related to the trees' location and that the effects from other biophysical processes are negligible. This assumption allowed us to interpolate contours of [CO₂F] over the spatial domain. Spatial interpolation plots of [CO₂F] in the UAM were established for five-year windows from 1980 to 2015 and for 2018 (the last year sampled). We used inverse distance weighting (IDW) (Legendre and Legendre 2012); a method based on the assumption that data with closer spatial proximity are more closely related than the more distant (Spokas *et al* 2003). Since the number of values to interpolate defines the quality of interpolation, the resulting contours are representative of the series. Spatial interpolation was established using R libraries for spatial analysis, including *sp*, *raster* (Bivand *et al* 2008), and *rgeos* (Bivand *et al* 2017).

We also estimated the uncertainty in the spatial interpolations by computing a map of standard deviations between 1980-2018 across the study site. First, we derived annual contour plots between 1980-2018 using the mixed-effects model and the IDW. Second, we derived the uncertainty map by plotting the standard deviation estimates for each pixel position.

4. Results

4.1 Dendrochronological analysis

The average period for the TRWs ranged from 1977 to 2018. Statistical parameters obtained during the cross-dating process confirmed the annual periodicity of the tree rings of *F. uhdei*. A total of 964 tree rings were measured. The mean TRWs was 6.20 mm, and the Gini coefficient was 0.23. The mean series intercorrelation was 0.41 ($p < 0.05$), suggesting that there is an adequate annual synchronization. The mean first-order autocorrelation was -0.06, the low and statistically non-significant shows that the rings width series are independent variables. The expressed population signal (EPS) was 0.97, overpassing the threshold of 0.85 (Speer 2010). The mean sensitivity (MS) was 0.43, and the signal-to-noise ratio (SNR) was 24.32. The MS and SNR are relatively high; this suggests that there should be one or more environmental variables involved in the variability observed in tree growth. See the residual chronology of *F. uhdei* in Appendix A. Appendix B shows the microscopic and macroscopic characteristics of the growth rings of *F. uhdei*.

4.2 Temporal patterns in radiocarbon and [CO₂F]

Mean radiocarbon concentrations ($\Delta^{14}\text{C}$) for all trees in the UAM between 1977 and 2018 were lower than the corresponding concentrations for the background air (Figure 1). The observed data showed a strong radiocarbon dilution (Suess effect), particularly from 1977 to 2005, and for the last part of the curve, between about 2011 and 2018. See radiocarbon values in Appendix C.

The computed [CO₂F] values showed high variability during the 41 years recorded by tree rings (Figure 2). The largest [CO₂F] values occurred between 1977 and 1985. However, during this period, a small sample size of ^{14}C measurements was obtained with only one ring per year in

1977 and 1978, or between 2 or 3 rings per year; hence the observed high standard deviations. Then, between 1986 y 2012 [CO₂F] values remained relatively stable; but from 2013 to 2018, they grew consistently reaching the highest observed values (Figure 2).

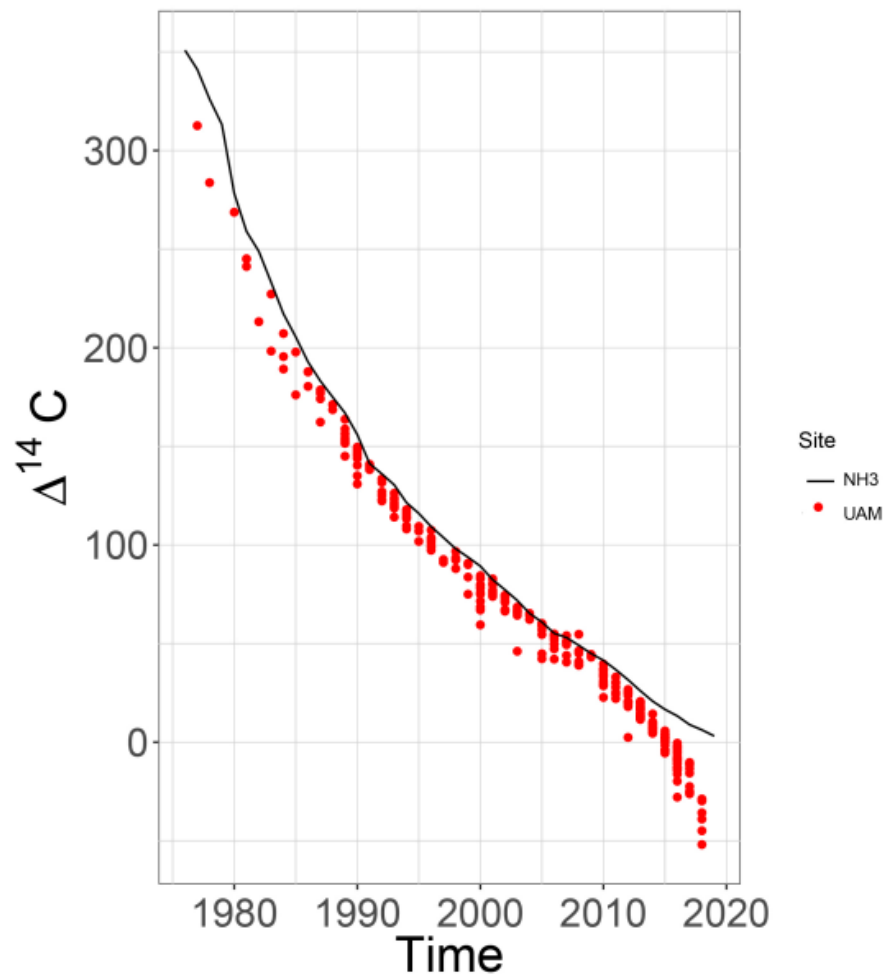


Figure 1: Radiocarbon concentration in the background air and in the measured tree rings expressed as $\Delta^{14}C$ (‰) over time. The red dots indicate the annual concentrations measured in the tree rings of *Fraxinus udhei* from the urban area of Medellín (UAM). The black line represents the background “clean air” concentration obtained from the North Hemisphere Zone 3 (NH3) curve.

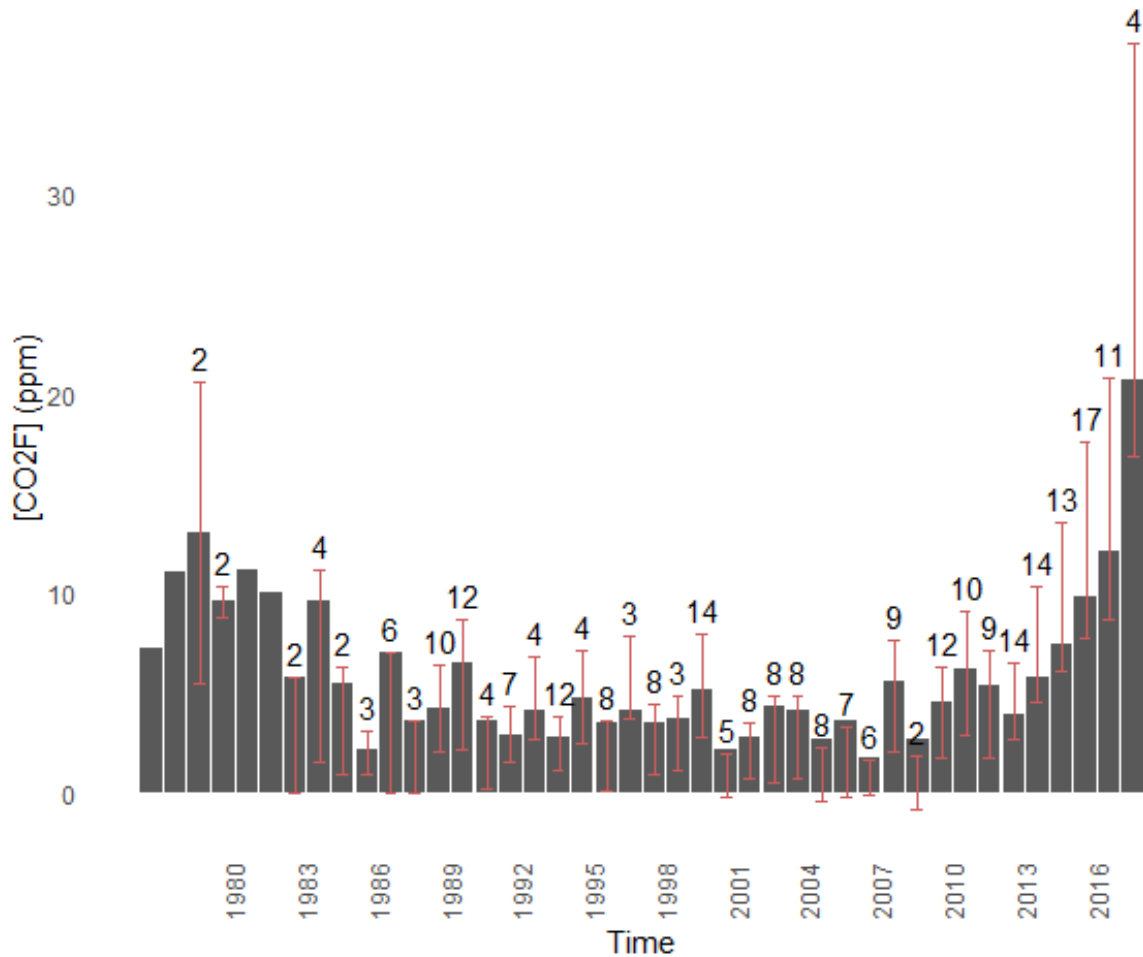


Figure 2: The concentration of fossil fuels CO₂ [COF] values over time in ppm for the urban area of Medellín between 1977 and 2018. The vertical bars indicate the standard deviation between tree rings. Numbers above the bars indicate the sample size for ¹⁴C analysis.

4.3 Comparison with emission data

The obtained [CO₂F] values compared relatively well with official CO₂ emission data reported for the UAM (Figure 3). Both the intercept and the slope of the linear model between the two variables were highly significant ($p < 2.5 \times 10^{-5}$). The coefficient of determination was 0.659. The obtained scatter plot exhibited some variability, with a higher density of points between 2000 and 2012 (Figure 3). Although the remaining five years are represented by a lower point density, they

spanned the entire regression domain, ensuring good confidence of the model parameters for at least the last 18 years of the study.

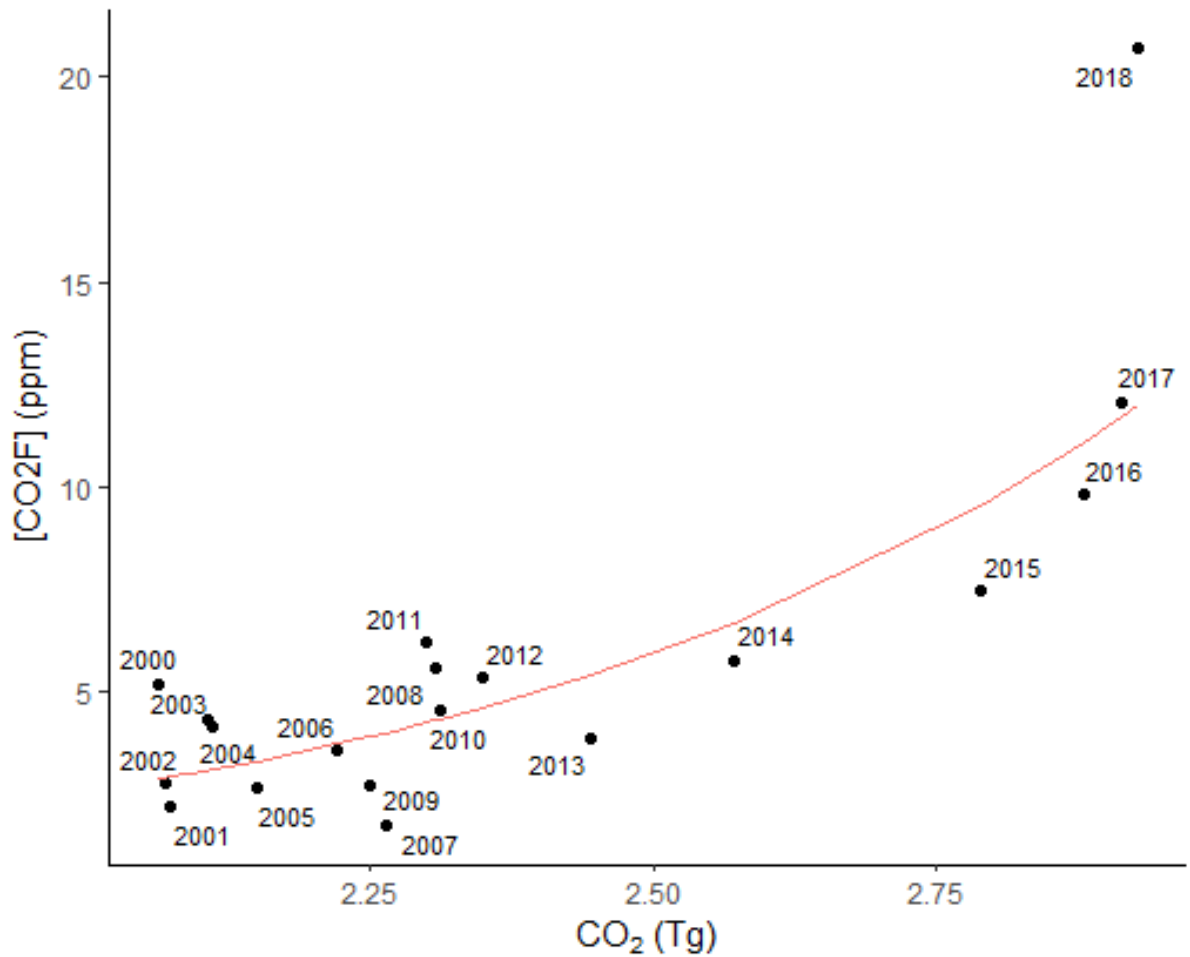


Figure 3: Comparison between average values of the concentrations of fossil fuels calculated in this study and official CO₂ emission data for the urban area of Medellín reported in official reports during the years 2000-2018. In this regression $p < 2.5 \times 10^{-5}$, $R^2 = 0.66$.

4.4 Time-series analysis

Fixed-effect parameters of the mixed model confirmed the polynomial trend of [CO₂F] over time (Table 1, *p-values*). Although the a_1 parameter estimate was not significant, the other two parameters estimated a parabolic trend. The regression fitted by the mixed-effects model shows upward concave quadratic behavior in the 35 trees sampled. For most trees (Figure 4), interpolations show that [CO₂F] values have decreased since the 1980s; they reached minimum values around the year 2000, to then increased until 2018. The importance of accounting for the tree-effect in the model is better appreciated by the difference in AIC values between the mixed model (AIC = 1419.801) versus the model without random effects (AIC = 1504.542), which differed significantly (Likelihood ratio = 96.741, $p < 0.001$) (Table 2). In addition, the residual standard deviation of the mixed model with random effects (Table 1, random effects sd = 2.336) was much smaller than that of the model without random effects (sd = 3.455).

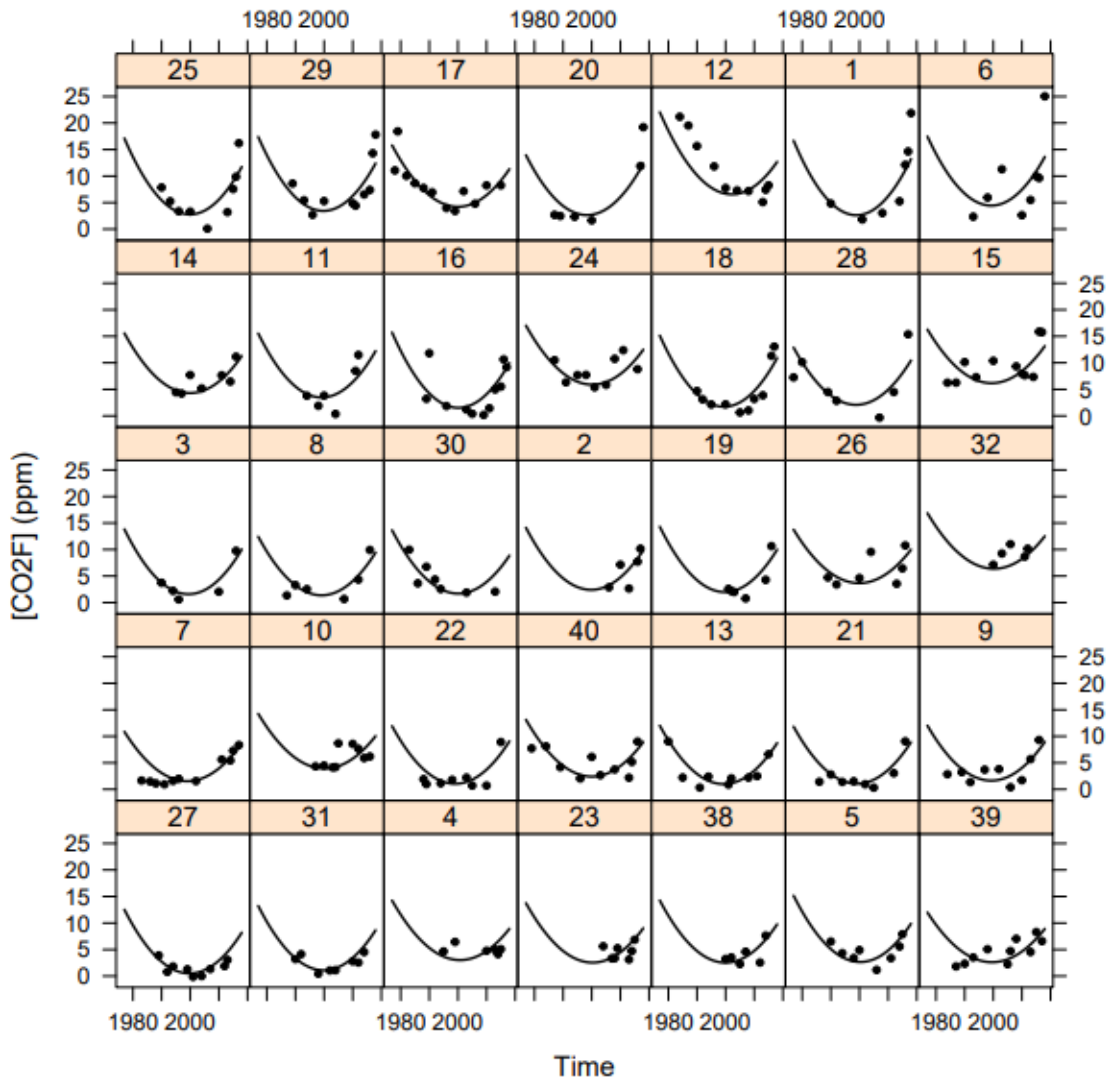


Figure 4: Mixed-effects model of the concentrations of fossil fuels CO₂ [CO₂F] over time. Each number indicates the tree code. The dots represent the calculated [CO₂F] data based on the ¹⁴C analyses made to each tree, and the lines represent predictions from the fixed-effect model.

In most trees, the quadratic function estimates a reduction of [CO₂F] in the tree rings during the 1980s and 1990s. They reach minimum values around the year 2000 and then increased consistently until 2018 (Figure 4).

Table 1: Parameter estimators of the mixed-effects model for the fossil-fuel CO₂ concentrations over time. The variables time and [CO₂F] represent the fixed effects, and the trees the random effects.

Fixed effects	Value	Standard error	t-value	p-value
a_0	5.584	0.354	15.759	0.000
a_1	9.978	5.033	1.983	0.049
a_2	39.763	4.851	8.197	0.000
Random effects	StdDev	Correlation		
a_{0s}	1.826			
a_{1s}	21.754	-0.414		
a_{2s}	20.241	0.130		
a_{0s}	2.336			

Table 2: ANOVA to compare the mixed-effects model (M1) and an equivalent model with no random effects (M0).

Model	df	AIC	BIC	logLik	L.Ratio	p-value
M1	10	1419.801	1456.22	-699.900		
M0	4	1504.542	1519.11	-748.271	96.714	<.0001

4.5 Spatial analysis

The spatial distribution of [CO₂F] in the UAM for a set of selected calendar years showed that fossil fuel emissions are not distributed homogeneously over the UAM. Some locations of the city have changed differently over time, with the highest values of [CO₂F] observed for the selected years 1980, 2015, and 2018 (Figure 5, blue gradient). The lowest values occurred between 1995 and 2000 (Figure 5, yellow-green gradient). Overall, the downtown area depicted at the center of the panels always had the highest values (Figure 5). Our space-time method revealed two hotspots of high [CO₂F] concentration in the UAM and their evolution between 1980 and 2018. One north from downtown, and another to the south (Figure 5, left). Similarly, and in agreement with the previous time series analysis, we observed that the temporal evolution of consistently decreased from 1980 to 2000 across the entire domain, and then consistently increased again until the last year of observation in 2018.

When we observe the UAM road mesh (Figure 5, right), several hotspots of high pollution of [CO₂F] (light green color, about 5 ppm) appear towards the downtown, north, and south. The main streets and avenues also present high pollution (light green color, about 5 ppm) and even higher values (blue color, about 15 ppm).

The uncertainties are in the range of 2.4 to 3.2 ppm (Figure 6), most of the uncertainties are less than 3 ppm. The points of greatest variability are defined by tree locality. There are 7 trees that are contributing the highest variability, which are mostly clustered around the downtown area of the UAM.

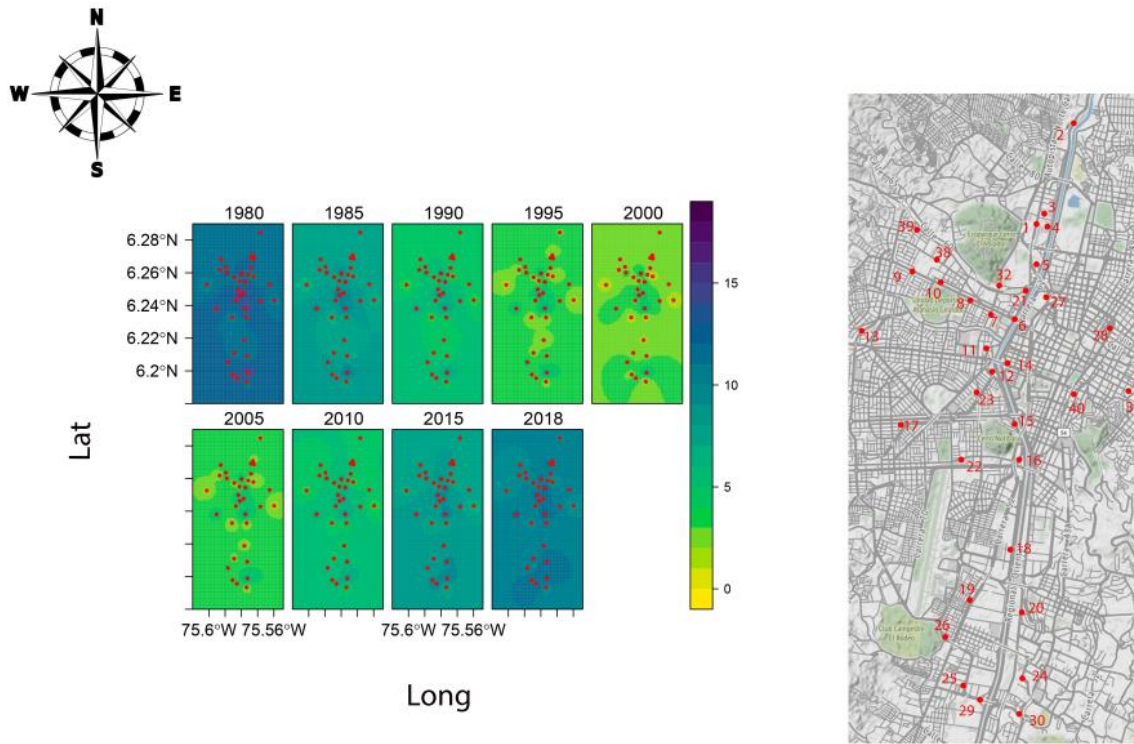


Figure 5: Spatial interpolation of fossil fuels concentrations [CO₂F] (scale bar in ppm) across the urban area of Medellín, in five-year windows between 1980-2015 and for the year 2018. Red dots in each window represent the location of the 35 trees of *F. uhdei*. On the right side is the urban area of Medellín city for the year 2020. The red dots are the 35 trees of *F. uhdei* with their respective code.

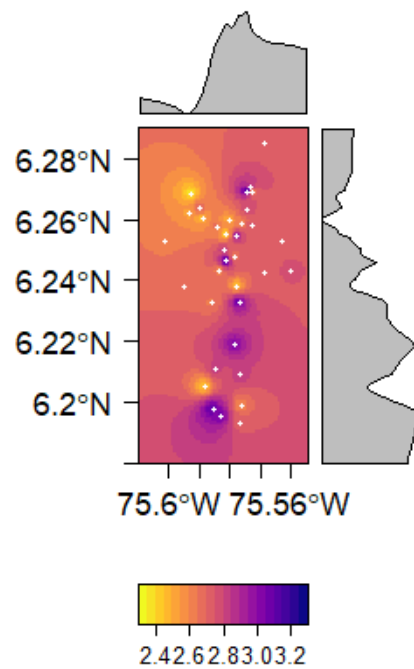


Figure 6: Uncertainty map of spatial interpolations of fossil fuel concentrations [CO₂F] (scale bar in ppm) across the urban area of Medellín, between 1980-2018; the white dots represent the location of the 35 trees of *F. uhdei*.

5. Discussion

Our results are consistent with previous studies based on radiocarbon analysis in tree rings of urban trees. All studies have found that the higher ^{14}C values correspond to cleaner fossil fuels pollution habitats from remote high elevation areas. In contrast, low values are associated with fossil fuels emissions in densely populated areas with larger-sized industrial and traffic footprints, corresponding to more polluted atmospheres.

This study demonstrates the utility of radiocarbon analysis in annual tree rings to reconstruct the spatial and temporal contribution of fossil fuels to the atmosphere of a city. It confirms the existence of annual rings in *F. uhdei* (Miranda-Áviles *et al* 2009, Villanueva Díaz *et al* 2015) outside its natural distribution range, and demonstrates its usefulness to study pollution by fossil fuels in cities, previously reported only for Mexico (Beramendi-Orosco *et al* 2013a).

An important novel aspect of our study is the use of a mixed-effects model, which allowed us to interpolate the [CO₂F] in years where we did not analyze ^{14}C , controlling for the variance of individual trees that are subject to specific levels of urban pollution. Our method allowed us to reconstruct spatially and temporally the mean values of [CO₂F] for 41 years at an annual resolution (Figure 5), with a robust quantification of prediction uncertainty (Figure 6), which is a measure of the variability due to (1) variability of atmospheric $^{14}\text{CO}_2$ values, and (2) uncertainty in growth rings and dating.

High variability in $^{14}\text{CO}_2$ can be attributed mainly to the heterogeneity of emission sources within the urban environment and to atmospheric transport from the Northern hemisphere through the dynamics of Intertropical Convergence Zone (ITCZ) (Ancapichún *et al* 2021, Hua *et al* 2021). In South America (SA), the ITCZ migrates annually from January to July from southern Brazil and northern Argentina towards the north. From July to January, it returns to the south. However, it leaves SA to the west through a narrow strip in the Pacific coast (Ancapichún *et al* 2021). This region of ITCZ activity exactly coincides with the SA domain of the Northern Hemisphere Zone 3 curve (Hua *et al* 2021) used in this study. The mean position of the ITCZ, where low pressures are present throughout the year, is located at about 4-5°N on the Colombian Pacific coast (Ancapichún *et al* 2021). Medellín, at about 6.2°N, is influenced by the ITCZ twice a year. Therefore, both winds from the southeast Amazon basin and from the northeastern savannas of

Venezuela transport air to Medellín. The ¹⁴C NH Zone 3 curve (Hua *et al* 2021) captures well these different sources of ¹⁴CO₂ to the background air.

The second source of variability in [CO₂F] can be explained by variability due to tree-ring growth and uncertainties in tree-ring dating. Our series intercorrelation was relatively low, although significant (0.41, $p < 0.05$), compared to three studies done in Mexico with the same species (from 0.44 to 0.49) (Miranda-Áviles *et al* 2009, Villanueva Díaz *et al* 2015). In the studies in Mexico, they eliminated between 18 and 68% of the series with the lowest correlation with the mean series. This is appropriate in dendroclimatic studies (Speer 2010) such as those previously cited. However, our study is dendrochemical, and eliminating series also means eliminating many ¹⁴C analysis. But there are other factors affecting the tree-rings width different to the climate in the environment of cities. These factors include high stress due to other pollutants and physical barriers imposed by cement and asphalt that limit the entry of water into the soil and the development of roots. Some of these trees may also be exposed to frequent mutilations of branches and large roots by repeated pruning. The bacterium '*Candidatus Phytoplasma asteris*' has been identified as causing yellowing of leaves and defoliation of *F. uhdei* in urban trees of Bogotá, Medellín, and other Colombian cities (Filgueira *et al* 2004, Perilla-Henao *et al* 2012). Although we try to select healthy trees with the naked eye, we can't discard that the effects of this disease could affect photosynthesis and induce variations in the width of the rings in some sampled trees. Also, during the early years, when the trees have plenty of light and ground space, the rings of *F. uhdei* in the UAM tend to be complacent (Figure 2 in Appendix B), with little difference in width. These effects make crossdating considerably more difficult and reduce serial intercorrelation even if the dating is correct.

Our quantification of uncertainty in the predictions (Figure 6) captures these differences sources of variability and helps to identify hotspots of variability in [CO₂F]. The uncertainty values of [CO₂F] that we obtained are of only a few ppm and suggest that the different sources of uncertainty mentioned in the previous paragraphs contribute only a small proportion to the total uncertainty in predictions.

The parabolic patterns revealed by the [CO₂F] values and captured by the model are challenging to interpret (Figures 4 and 5). They could be explained by numerous reasons, ranging

from changes in the local distribution of emission sources to global economic factors affecting oil prices and local consumption. For instance, the second oil crisis in 1979, which increased international oil prices by about a factor of five, may have reduced oil consumption. However, we were not able to document this in Colombia where oil production is state-owned, because oil prices depend on many factors, including state subsidies. Globally, the response to high fossil fuel prices included the use of alternative energy sources such as carburant alcohol, and the construction of compact vehicles with smaller engines and lower fuel consumption, among other measures tending to diversify the energy basket ⁴ (Lee 1979). Combined, these efforts resulted in a decline in daily oil consumption worldwide in the six years following the crisis⁴. Likewise, between 1980 and 2000 the population of Medellín grew from about one to about two million people. Then, both fixed and mobile sources of CO₂ of the UAM increased (Toro *et al*/2013, 2015, 2017, 2018). Why then did the [CO₂F] values decrease from 1977 to 1985? One potential explanation may have to do with the small number of observations for the early years in our record. The available ¹⁴C analysis were only done in one to three tree rings per year (Figures 1 and 2). Therefore, the number of tree rings sampled for this period might not have been sufficiently representative. After 1985, the number of tree rings analyzed was higher, which reduced uncertainty (Figures 1 and 2). All the oldest trees sampled were found in one of the most polluted areas, north of the downtown city (Figure 5). Another possible explanation for the high [CO₂F] values found may be related to the elevated industrial activity and particular topographic conditions of the Aburrá valley where the UAM is seated: two mountain ranges that block air currents and only allow the winds from the north (Bedoya and Martínez 2009, Correa *et al* 2009).

Medellín limits the north to the industrial Bello city with over five hundred thousand people, from which it is separated only by a street. Therefore, its pollutants are blown into the UAM by the wind. These pollutants are stored mainly in the tree rings north of the UAM.

The decrease in [CO₂F] values from 1990 to 2000 might also be related to local and global scale socio-economic factors. At the local level, it is relevant to mention the withdrawal of heavy industries from the UAM. This is the case of the metallurgic company Siderúrgica de Medellín and

⁴ <https://www.investopedia.com/terms/1/1979-energy-crisis.asp>

the Argos cement plant, among other heavy industries (Molina 2013). From this industrial area emerged a residential area with parks and museums. At the end of 1995, the Medellín Metro was inaugurated, providing a massive scale transportation system. On a global scale, some factors may have played a role in the [CO₂F] decrease. Such was the energy crisis of 1990 (“The Gulf War”) with the subsequent increase in fossil fuel prices and decrease in consumption. Also, during the 1990s, the transition from the carburetor to injection systems began in most engines, increasing efficiency in fuel consumption.

In contrast, from 2000 to 2018, the [CO₂F] increased considerably (Figures 4 and 5). Something expected because the vehicle fleet increased, and the population grew from about two million in 2000 to 2.5 million in 2018. This increase does not appear to be significantly affected by the global financial crisis of 2008 nor by the high oil prices induced by the "Arab Spring" between 2010 and 2012. No local policies managed to bend the upward curve of [CO₂F] in the last decades, namely: restrictions on mobility adopted by the city in 2001, the expansion of the Metro (2004, 2008, and 2016), or the implementation of transport by cables and electric trams.

Our research is unique in many respects compared to previous studies of fossil fuels pollution in urban areas using tree rings and the Suess effect: (1) Despite having done the highest number of ¹⁴C analysis in the tree rings so far (282 analysis), in comparison to those carried out in any previous study, we did not analyze the ¹⁴C in all tree rings of our study. However, our interpolation method allowed us to assign to each ring a value of [CO₂F]. (2) Our method integrates the [CO₂F] of all the rings to temporarily reconstruct with annual resolution the fossil fuels pollution in the UAM for 41 years, and spatially during the same period. The few temporal and spatial pollution reconstructions with tree rings found in the literature (Djuricin *et al* 2012, Sensula *et al* 2018, Hou *et al* 2020) do not have a method that integrates the ¹⁴C analysis of the rings in the sampled space. They are individually presented tree by tree. The number of trees sampled was also much lower (between 5 and 15 trees) despite representing larger and more populated metropolitan areas, such as Xi'an (Hou *et al* 2020) and the Los Angeles basin (Djuricin *et al* 2012), which largely overpasses 10 million people. (3) This study is likely the only spatial and temporal reconstruction of fossil fuel pollution using annual tree rings in the tropics, where it is often believed trees produce no annual rings. Regarding temporal reconstructions in the tropics, four

have been done in Mexico: three in Mexico City (Beramendi-Orosco *et al* 2015, 2017, Flores *et al* 2017), at 19°N, and the other in San Luis de Potosí, at 22°N (Beramendi-Orosco *et al* 2013b). That is, in the transition between tropics and subtropics. We found another study in Arequipa, Peru, at 16°S (Pazdur *et al* 2007, Quarta *et al* 2007). Each one of these studies used a single tree for each city. Using only a tree is the most common practice around the world. (4) Temporarily, only one study exceeded the 41 years of our study; one hundred years in a *Quercus* tree in New York City (Cain 1978). Other studies have exceeded 41 years but analyzed the rings discontinuously. (5) The 35 trees sampled in the UAM greatly exceed all the studies consulted, and generally, in a smaller and less populated area than most of them. This implies that our spatial and temporal reconstruction is finer than previously cited. (6) In these studies, the most used species are conifer trees, mostly *Pinus* spp. Only (Beramendi-Orosco *et al* 2013a), and this study, Jeřkovský *et al* (2015), and Cain (1978), used dicot trees: *F. uhdei*, *Tilia europea*, and *Quercus* sp, respectively. Overall, our method to integrate multiple trees with rigorous crossdating, a long chronology, frequent ring sampling, measurements of radiocarbon only in the α -cellulose on late wood, and statistical interpolations in space and time, allowed us to produce a reconstruction that is unique among all previous studies.

The methodology introduced in this study to reconstruct spatial and temporal patterns of [CO₂F] could be useful for many other cities. Records of CO₂ emissions, if they exist for some cities, do not have a spatial resolution that would allow one to identify regions or neighborhoods with large pollution sources. Trees serve as an important living archive that spreads over entire metropolitan areas. The obtained information is almost impossible to capture with a network of atmospheric observations. The reconstructed records of [CO₂F] can be used to evaluate the effectiveness of policies to reduce emissions or to identify hotspots of pollution that require special attention. These estimates can also serve as independent records to confirm or validate official reports on fossil fuel emissions.

We believe the equation reported by others (Rakowski *et al* 2008a, Beramendi-Orosco *et al* 2017), based on the mass balance equations of Levin *et al* (1989, 2003), is probably wrong. We recommend using our equations (10 and 12) depending on the required variables. It should be used equation (10) when CO₂ concentration in the study area has been measured. But, if this concentration is unknown, background CO₂ concentration is known, equation (12) should be used.

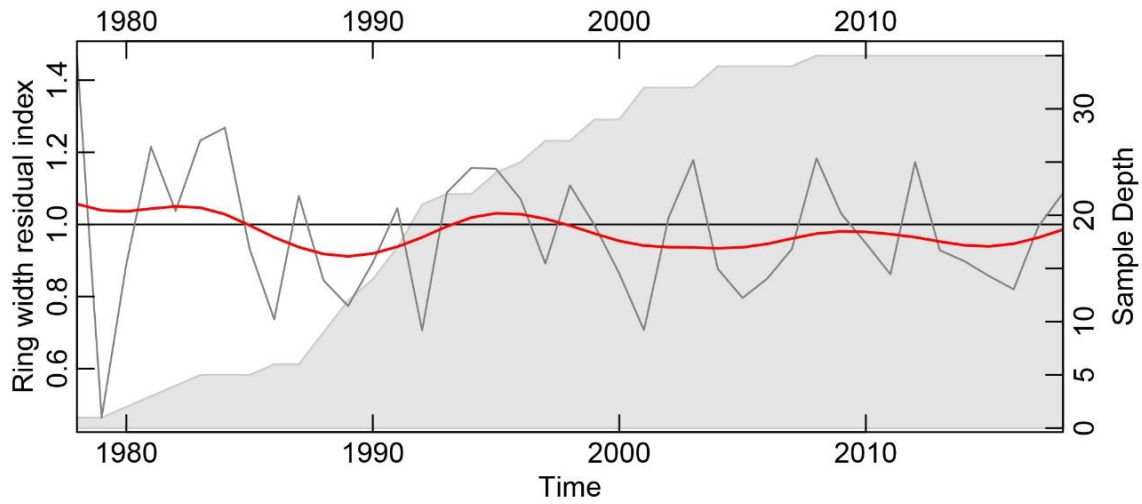
6. Conclusions

By using a combination of dendrochronological analysis, radiocarbon measurements in tree rings, and statistical modelling, we reconstruct spatially and temporally the contribution of fossil fuel carbon to the atmosphere of the urban area of Medellín, Colombia. This reconstruction, which spans from 1977 to 2018, identified hotspots of emissions related to traffic and industrial areas as well as urban population growth. We identified an increase in the contribution of fossil fuel carbon to atmospheric CO₂ in the last decades, and recent efforts from local authorities to reduce traffic and emissions do not seem to have a distinguishable effect on [CO₂F]. The method we developed here could be of tremendous utility for reconstructing the history of fossil fuel emissions in many other cities and identifying hotspots. This method provides valuable information for the planning and evaluation of measures to reduce emissions in urban areas.

In this study, possible errors were found in the derivation of a widely used equation for studying air pollution by fossil fuels, based on the mass balance equations of Levin *et al* (1989, 2003). Here we propose two alternative equations depending on the known or measured variables of CO₂ concentrations.

7. Appendix A: Residual chronology

The residual tree-ring widths chronology of thirty-five of *Fraxinus uhdei* trees in the urban area of Medellín (grey line) and the sample depth (gray shaded area).



8. Appendix B: Tree ring descriptions

The rings of *Fraxinus uhdei* are defined at the beginning by very large pores that later reduce in size (semi-ring-porous rings), and by parenchyma bands and slight change in density with smaller and thicker fibers towards the end of the rings.

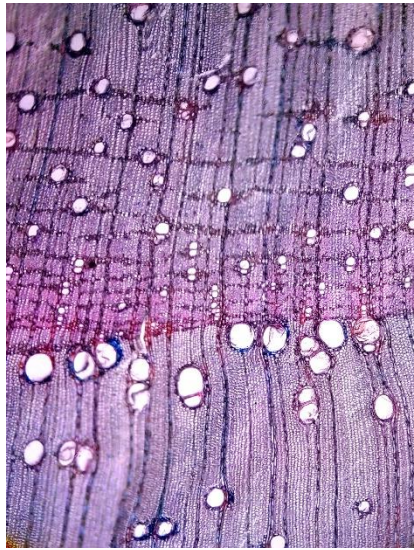


Figure 1: Transversal cut on the microtome of the tree rings of *Fraxinus uhdei*.



Figure 2: Tree rings of *Fraxinus uhdei*. Complacent growth rings during the first years in *F. uhdei*. The six complete rings have a mean sensitivity (MS) of 1.16. If they were all the same width, then MS = 1.

9. Appendix C: Radiocarbon values

Table 1: Radiocarbon values for *Fraxinus uhdei* tree-ring samples from urban area of Medellín.

Tree Code	Year	$\Delta^{14}\text{C}$	err
1	1990	140.4	2.9
1	2001	77.1	2.5
1	2008	40.9	2.8
1	2014	7.5	2.7
1	2016	-16.2	2.5
1	2017	-26.2	2.4
1	2018	-44.9	2.4
2	2006	47.3	2.6

Tree Code	Year	$\Delta^{14}\text{C}$	err
2	2010	22.7	1.7
2	2013	19.2	2.7
2	2016	-5.7	2.6
2	2017	-15.7	2.5
3	1990	143.9	2.9
3	1994	114.6	1.6
3	1996	107.5	2.5
3	2010	36	3
3	2016	-10.6	2.4
4	1995	101.8	2.6
4	1999	75	2.6
4	2010	28.9	2.8
4	2013	13.4	4
4	2014	10.3	2.6
4	2015	3.9	2.4
5	1990	135.1	4.4
5	1994	108.1	4.1
5	1998	88	4
5	2000	75	4.1
5	2006	52	2.4
5	2011	27.9	2.4
5	2014	6.7	2.4
5	2015	-3	2.5
7	1983	227.2	4.5
7	1986	187.7	4.4
7	1988	171.2	4.5
7	1991	138.2	4.4
7	1994	116.5	1.5
7	1996	103.3	4.3
7	2002	72.8	4.2
7	2011	22.1	4

Tree Code	Year	$\Delta^{14}\text{C}$	err
7	2014	7	3.9
7	2015	-1.5	2.4
7	2017	-11.4	2.4
9	1984	207.2	4.7
9	1989	156.3	4.7
9	1992	131.7	2.1
9	1997	92.6	2.2
9	2002	66.4	1.9
9	2006	54.1	2.2
9	2010	36.9	2.3
9	2013	11.5	2.1
9	2016	-9.5	2
13	1980	245.1	2.3
13	1985	197.8	2.4
13	1991	140.2	2.5
13	1994	114	2.3
13	2001	79.8	2.3
13	2002	71.3	2.1
13	2008	43.1	2.2
13	2011	30.2	2.4
13	2015	0.1	2.6
16	1989	156.4	2.9
16	1990	118.7	3
16	1996	103.7	2.9
16	2003	68.5	2.8
16	2005	59.8	2.7
16	2009	44.5	2.7
16	2011	33	2.6
16	2013	13.3	2.6
16	2015	2.8	2.6
16	2016	-12.7	2.7
16	2017	-13.4	2.3
18	1990	140.9	2.1

Tree Code	Year	$\Delta^{14}\text{C}$	err
18	1992	126.2	2.6
18	1995	109.4	2.6
18	2000	82.9	1.9
18	2005	59.1	1.9
18	2008	46.3	1.8
18	2010	33	2.1
18	2013	16.1	1.9
18	2016	-14.3	1.9
18	2017	-22.5	2.3
19	2001	74.9	1.6
19	2002	71	2
19	2003	66.2	1.8
19	2007	50.9	2.5
19	2014	9.9	1.8
19	2016	-12.7	2.4
25	1990	130.9	2.3
25	1993	114.1	2
25	1996	99.1	2
25	2000	79.6	2.1
25	2006	54.9	2
25	2013	17.8	1.8
25	2015	-2.2	1.9
25	2016	-10.9	1.9
25	2017	-29.8	1.9
26	1989	151.5	2.1
26	1992	125.2	2.2
26	2000	75.8	2
26	2004	39	2.1
26	2013	16.9	2.1
26	2015	0.5	1.9
26	2016	-13	2

Tree Code	Year	$\Delta^{14}\text{C}$	err
27	1989	154.2	2.2
27	1992	133.5	2.2
27	1994	115.8	2.2
27	1999	90	2.2
27	2001	82.8	2
27	2004	65.3	2
27	2007	49.4	1.9
27	2012	26.7	1.9
27	2013	18.2	1.9
31	1990	145.6	2.1
31	1992	123	2.1
31	1998	96.7	1.5
31	2002	74.2	2
31	2004	62.2	1.9
31	2010	34.1	1.9
31	2012	25	1.8
31	2014	9.3	2.1
38	2000	79.8	2
38	2002	67.2	2
38	2005	54.6	1.8
38	2007	40.6	2
38	2012	25	1.8
38	2014	1.6	1.8
40	1979	283.7	2.3
40	1984	189.2	2.2
40	1989	153.3	2.1
40	1996	103.1	2.1
40	2000	71.5	2
40	2003	64.3	2
40	2008	39	1.6
40	2013	20.4	1.6
40	2014	7.7	2
40	2016	-8.8	1.8

Tree Code	Year	$\Delta^{14}\text{C}$	err
22	1988	168.6	2.8
22	1989	163.7	2
22	1994	117.9	2.1
22	1998	92.7	1.6
22	2003	65.6	2.2
22	2005	58.9	2.6
22	2010	39.6	2.4
22	2015	-5.5	3.2
21	1986	187.9	1.9
21	1990	146.9	1.8
21	1994	117.1	1.8
21	1998	93.5	1.8
21	2002	74.5	1.7
21	2005	60	1.7
21	2012	23.7	1.7
21	2016	-8.9	1.8
23	2004	49.7	1.8
23	2007	44	1.7
23	2008	40	1.7
23	2009	31	1.7
23	2013	18	1.7
23	2014	8.8	1.8
23	2015	-0.5	1.8
24	1987	148.6	1.8
24	1991	121.3	1.8
24	1995	92.7	1.8
24	1998	75.4	1.8
24	2001	66.9	1.7
24	2005	44.8	1.8
24	2008	20.6	1.8
24	2011	5	1.8

Tree Code	Year	$\Delta^{14}\text{C}$	err
24	2016	-8.3	1.7
28	1977	312.6	2
28	1980	241.2	2.2
28	1989	152.3	1.9
28	1992	127	2.1
28	2007	54	4.5
28	2012	20	1.8
28	2017	-27.9	1.7
29	1989	139.2	1.8
29	1993	113.5	1.8
29	1996	101.1	1.8
29	2000	73.9	2
29	2010	28.6	1.8
29	2011	25.2	1.8
29	2014	4.3	1.7
29	2016	-4.9	1.8
29	2017	-25.4	1.7
29	2018	-35.8	1.7
30	1983	198.3	2.1
30	1986	180.4	1.9
30	1989	145	1.8
30	1992	122.3	1.8
30	1994	113.5	1.8
30	2003	66.5	3.1
30	2013	20.7	1.8
32	2000	68.6	2
32	2003	46.1	1.9
32	2006	25.6	1.8
32	2011	14.3	1.8
32	2012	5.7	1.8
39	1987	177	2.2
39	1990	148.4	1.8
39	1993	119.5	1.9

Tree Code	Year	$\Delta^{14}\text{C}$	err
39	1998	83.1	1.9
39	2005	54.7	1.7
39	2006	42.3	1.8
39	2008	30.3	1.7
39	2013	14.4	1.7
39	2015	-4	1.7
39	2017	-7.2	1.8
6	1993	123.1	2
6	1998	80.5	1.8
6	2003	40.6	2
6	2010	34.5	1.9
6	2013	12	1.8
6	2015	-8.1	1.7
6	2016	-10.3	2
6	2018	-51.9	3.6
8	1987	178.6	2.2
8	1990	145.3	1.9
8	1994	113.6	2
8	2007	51.2	2
8	2012	20.4	2
8	2016	-11	1.8
10	1997	90.7	1.9
10	2000	76.2	1.9
10	2003	60.2	1.9
10	2004	53.6	2
10	2005	37.2	1.9
10	2010	19.1	1.7
10	2012	12	1.8
10	2014	5.9	1.8
10	2016	-2	1.8
11	1994	109.7	1.9

Tree Code	Year	$\Delta^{14}\text{C}$	err
11	1998	92.4	1.9
11	2000	78.1	1.8
11	2004	64.3	1.7
11	2011	14.8	1.7
11	2012	2.4	1.7
12	1984	146.7	1.8
12	1987	120.5	1.8
12	1990	107	1.9
12	1996	74.3	1.8
12	2000	66.9	1.9
12	2004	45.1	1.7
12	2008	29.9	1.7
12	2013	13	1.9
12	2014	2.1	1.7
12	2015	-3.9	2
14	1995	102.4	2.2
14	1997	91.1	2.2
14	2000	67	2
14	2004	50.9	2
14	2011	16.9	2
14	2014	4.5	2
14	2016	-13.9	1.8
15	1984	195.5	1.9
15	1987	162.3	1.9
15	1990	123.8	1.8
15	1994	99.1	2
15	2000	59.5	1.8
15	2008	24.3	1.8
15	2010	20.6	1.8
15	2011	16.9	1.8
15	2014	2.3	1.8
15	2016	-25	1.7
15	2017	-28.8	1.7

Tree Code	Year	$\Delta^{14}\text{C}$	err
17	1978	283.7	2
17	1979	245	2
17	1982	213.2	2.1
17	1985	176.1	1.8
17	1988	149.6	2
17	1991	119.4	1.8
17	1996	97.3	1.8
17	1999	83.7	1.9
17	2002	57	1.9
17	2006	42.1	1.7
17	2010	19.9	1.8
17	2015	-3.9	1.8
20	1987	174.1	1.9
20	1989	158.8	1.9
20	1994	114.2	2
20	2000	84.4	1.7
20	2017	-19.8	1.6
20	2018	-39	1.8

10. References

- Affek H, Xu X and Eiler J 2007 Seasonal and diurnal variations of ^{13}C ^{18}O ^{16}O in air: Initial observations from Pasadena, CA Hagit *Geochim. Cosmochim. Acta* **71** 5033–43
- Aguilera-Betti I, Lucas C, Ferrero M E and Muñoz A A 2020 A Network for Advancing Dendrochronology, Dendrochemistry and Dendrohydrology in South America *Tree-Ring Res.* **76** 94–101
- Alberte R S, McClure P R and Thornber J P 1976 Photosynthesis in trees *Plant Physiol.* **58** 341–4
- Ancapichún S, De Pol-Holz R, Christie D A, Santos G M, Collado-Fabbri S, Garreaud R, Lambert F, Orfanoz-Cheuquelaf A, Rojas M, Southon J, Turnbull J C and Creasman P P 2021 Radiocarbon bomb-peak signal in tree-rings from the tropical Andes register low latitude atmospheric dynamics in the Southern Hemisphere *Sci. Total Environ.* **774** 145126
Online: <https://doi.org/10.1016/j.scitotenv.2021.145126>
- Balouet J C, Oudijk G, Smith K T, Petrisor I, Grudd H and Stocklassa B 2007 Applied dendroecology and environmental forensics. Characterizing and age dating environmental releases: Fundamentals and case studies *Environ. Forensics* **8** 1–17
- Bancone C E P, Turner S D, Ivar do Sul J A and Rose N L 2020 The Paleoecology of Microplastic Contamination *Front. Environ. Sci.* **8** 1–20

-
- Battipaglia G, Marzaioli F, Lubritto C, Altieri S, Strumia S, Cherubini P and Cotrufo M F 2010 Traffic pollution affects tree-ring width and isotopic composition of *Pinus pinea* *Sci. Total Environ.* **408** 586–93 Online: <http://dx.doi.org/10.1016/j.scitotenv.2009.09.036>
- Beaudon E, Gabrielli P, Sierra-hernández M R, Wegner A and Thompson L G 2017 Central Tibetan Plateau atmospheric trace metals contamination : A 500-year record from the Puruogangri ice core *Sci. Total Environ.* **601–602** 1349–63 Online: <http://dx.doi.org/10.1016/j.scitotenv.2017.05.195>
- Bedoya J and Martínez E 2009 Calidad del aire en el valle de Aburrá Antioquia-Colombia *Dyna* **76** 7–15
- Beramendi-Orosco L E, Gonzalez-Hernandez G, Martinez-Jurado A, Martinez-Reyes A, Garcia-Samano A, Villanueva-Diaz J, Javier Santos-Arevalo F, Gómez-Martínez I and Amador-Muñoz O 2015 Temporal and spatial variations of atmospheric radiocarbon in the Mexico City Metropolitan Area *Radiocarbon* **57** 363–75
- Beramendi-Orosco L E, González-Hernández G, Martínez-Reyes A, Morton-Bermea O, Santos-Arévalo F J, Gómez-Martínez I and Villanueva-Díaz J 2017 Changes in CO₂ emission sources in Mexico city metropolitan area deduced from radiocarbon concentrations in tree rings *Radiocarbon* 1–4
- Beramendi-Orosco L E, Hernández-Morales S, González-Hernandez G, Constante-Garcia V and Villanueva-Díaz J 2013a Dendrochronological potential of *Fraxinus uhdei* and its use as bioindicator of fossil CO₂ emissions deduced from radiocarbon concentrations in tree rings *Radiocarbon* **55** 833–40
- Beramendi-Orosco L E, Rodriguez-Estrada M ., Morton-Bermea O, Romero F, González-Hernandez G and Hernández-Alvarez E 2013b Correlations between metals in tree-rings of *Prosopis juliflora* as indicators of sources of heavy metal contamination *Appl. Geochemistry* **39** 78–84 Online: <http://dx.doi.org/10.1016/j.apgeochem.2013.10.003>
- Berg M, Thi P, Trang K, Stengel C, Buschmann J, Hung P, Dan N Van, Giger W and Stüben D 2008 Hydrological and sedimentary controls leading to arsenic contamination of

- groundwater in the Hanoi area , Vietnam : The impact of iron-arsenic ratios , peat , river bank deposits , and excessive groundwater abstraction *Chem. Geol.* **249** 91–112
- Berlage H P 1931 Over het verband tusschen de dikte der jaarringen van djatiboomen (*Tectona grandis* L. f.) en den regenval op Java *Tectona* **24** 939–53
- Binda G, Di Iorio A and Monticelli D 2021 The what, how, why, and when of dendrochemistry: (paleo)environmental information from the chemical analysis of tree rings *Sci. Total Environ.* **758** 143672 Online: <https://doi.org/10.1016/j.scitotenv.2020.143672>
- Bivand R, Pebesma E J and Gómez-Rubio V 2008 *Applied Spatial Data Analysis with R* ed Springer Online: [papers2://publication/uuid/602A78BA-C239-4615-9538-633DA46454D9](https://doi.org/10.1007/978-1-4020-8837-6)
- Bivand R, Rundel C, Pebesma E, Stuetz R and Hufthammer K O 2017 Package 'rgeos'. Interface to Geometry Engine - Open Source ('GEOS') 77
- Bowman S 1990 *Radiocarbon dating* vol 1 (University of California Press)
- Brandis D 1979 Memorandum of the rate of growth of teak *Indian For.* **4** 215–25 Online: <http://www.sciencedirect.com/science/article/pii/S0160738315000444><http://www.sciencedirect.com/science/article/pii/S0160738315000444><http://eprints.lancs.ac.uk/48376/%255Cnhttp://dx.doi.org/10.1002/zamm.19630430112%25Ahttp://www.sciencedirect.com/>
- Brandis D 1960 *Report on the teak forests of Pegu, with a memorandum on the teak in the Tharawaddy forests* (London: Printed by George Edward Eyre and William Spotteswoody) Online: <http://www.sciencedirect.com/science/article/pii/S0160738315000444>
- Brienen R J W, Schöngart J and Zuidema P A 2016 Tree rings in the tropics: insights into the ecology and climate sensitivity of tropical trees *Tropical tree physiology* ed S Goldstein G. (Springer) pp 439–61
- Bunn A G 2008 Statistical and visual crossdating in R using the dplR library *Dendrochronologia* **28** 251–8 Online: <http://dx.doi.org/10.1016/j.dendro.2009.12.001>
- Burken J G, Vroblesky D A and Balouet J C 2011 Phytoforensics, dendrochemistry, and phytoscreening: New green tools for delineating contaminants from past and present

Environ. Sci. Technol. **45** 6218–26

- Busch F A, Holloway-Phillips M, Stuart-Williams H and Farquhar G D 2020 *Revisiting carbon isotope discrimination in C₃ plants shows respiration rules when photosynthesis is low* vol 6
- Cain W F 1978 Carbon-14, tree rings, and urban air pollution *Environ. Int.* **1** 167–71
- Capano M, Marzaioli F, Sirignano C, Altieri S, Lubritto C, D'Onofrio A and Terrasi F 2010 ¹⁴C AMS measurements in tree rings to estimate local fossil CO₂ in Bosco Fontana forest (Mantova, Italy) *Nucl. Instruments Methods Phys. Res. Sect. B Beam Interact. with Mater. Atoms* **268** 1113–6 Online: <http://dx.doi.org/10.1016/j.nimb.2009.10.112>
- Cesur A, Zeren Cetin I, Abo Aisha A E S, Alrabiti O B M, Aljama A M O, Jawed A A, Cetin M, Sevik H and Ozel H B 2021 The usability of *Cupressus arizonica* annual rings in monitoring the changes in heavy metal concentration in air *Environ. Sci. Pollut. Res.* **28** 35642–8
- Cook E R and Kairiukstis L A 1990 *Methods of dendrochronology. Applications in the Environmental Sciences* (Springer Netherlands)
- Correa M, Zuluaga C, Palacio C, Pérez J and Jiménez J 2009 Acoplamiento de la atmósfera libre con el campo de vientos locales en una región tropical de topografía compleja. Caso de estudio: valle de Aburrá, Antioquia, Colombia *Dyna* **76** 17–27
- Coster C 1927 Zur anatomie und physiologie der zuwachszone-und jahresringbildung in den tropen *Ann. Jard. Bot. Buitenzorg* **38** 1–114
- Coster C H 1926 Die Buche auf dem Gipfel des Pangerango *Ann. Jard. Bot. Buitenzorg* **35** 105–19
- Coster C H 1923 Lauberneuerung und andere periodische Lebensprozesse in dem trockenen Monsun-Gebiet OstJava's *Ann. Jard. Bot. Buitenzorg* **33** 117–88 Online: <http://www.sciencedirect.com/science/article/pii/S0160738315000444>
- Cutter B E and Guyette R P 1993 Anatomical, chemical, and ecological factors affecting tree

species choice in dendrochemistry studies *Env. Qual* **22** 611–9

D'Arcy F, Boucher É, De Moor J M, Hélie J F, Piggott R and Stix J 2019 Carbon and sulfur isotopes in tree rings as a proxy for volcanic degassing *Geology* **47** 825–8

Deepak M S, Sinha S K and Rao R V 2010 Tree-ring analysis of teak (*Tectona grandis* L. f.) from Western Ghats of India to determine drought years *Emirates J. Food Agric.* **22** 388–97

Djuricin S, Pataki D E and Xu X 2010 A comparison of tracer methods for quantifying CO₂ sources in an urban region *J. Geophys. Res. Atmos.* **115** 1–13

Djuricin S, Xu X and Pataki D E 2012 The radiocarbon composition of tree rings as a tracer of local fossil fuel emissions in the Los Angeles basin : 1980 – 2008 *J. Geophys.* **117** 1–15

Dong M, Chen W, Chen X, Xing X, Shao M, Xiong X and Luo Z 2021 Geochemical markers of the Anthropocene: Perspectives from temporal trends in pollutants *Sci. Total Environ.* **763** 142987 Online: <https://doi.org/10.1016/j.scitotenv.2020.142987>

Dongarrà G and Varrica D 2002 $\delta^{13}\text{C}$ variations in tree rings as an indication of severe changes in the urban air quality *Atmos. Environ.* **36** 5887–96

Douglass A 1941 Crossdating in Dendrochronology *J. For.* **39** 825–31

Douglass A 1909 Weather cycles in the growth of big trees *Mon. Weather Rev.* **37** 225–37

Durgante F 2017 *Protocolo de extração de celulose e branqueamento da madeira utilizada por Durgante 2017 para datação ^{14}C* (Manaus: Instituto Nacional de Pesquisas da Amazônia Coordenação)

Figueira R, Sérgio C and Sousa A J 2002 Distribution of trace metals in moss biomonitors and assessment of contamination sources in Portugal *Environ. Pollut.* **118** 153–63

Filgueira J J, Franco-Lara L, Salcedo J E, Gaitan S L and Boa E R 2004 Urapan (*Fraxinus udhei*) dieback, a new disease associated with a phytoplasma in Colombia *Plant Pathol.* **53** 520

Flores J A, Solís C, Huerta A, Ortiz M E, Rodríguez-Ceja M G, Villanueva J and Chávez E 2017

Historic binnacle of ¹⁴C/¹²C concentration in Mexico city *Phys. Procedia* **90** 2–9 Online:
<http://dx.doi.org/10.1016/j.phpro.2017.09.007>

Geiger F 1915 Anatomische Untersuchungen u ber die Jahresringbildung von *Tectona grandis*.
Jahrb *Wiss. Bot* **55** 521–607 Online:
<http://eprints.lanccs.ac.uk/48376/%5Cnhttp://dx.doi.org/10.1002/zamm.19630430112%0Ahttp://www.sciencedirect.com/science/article/pii/S0160738315000444%0Ahttp://www.ncbi.nlm.nih.gov/pubmed/25926610%5Cnhttp://www.pubmedcentral.nih.gov/articlerender.fcgi?artid>

Giraldo J A 2021 *Annual tree rings in the rainiest forests of the americas* (Universidad Nacional de Colombia.) Online: <https://repositorio.unal.edu.co/handle/unal/80415>

Graven H, Keeling R and Rogelj J 2020 Changes to Carbon Isotopes in Atmospheric CO₂ Over the Industrial Era and Into the Future Global Biogeochemical Cycles *Glob. Biog* **34** 1–21
Online: <https://doi.org/10.1029/2019GB006170%0AReceived>

Grubler A, Johansson T, Mundaca L, Nakicenovic, Pachauri S, Riahi K, Rogner H and Strupeit L 2012 Chapter1. Energy primer *Global Energy Assessment (GEA)* p 118

Guibal F and Guiot J 2020 Dendrochronology *Paleoclimatology* pp 117–22

Hartig G L 1795 *Anweisung Zur Taxation der Forste, Oder Zur Bestimmung Des Holzer-Trags Der Walder: Ein Beytrag Zur Hoheren Forstwissenschaft* (Giessen, Darmstadt: Heyer, Stahl) Online: <http://www.sciencedirect.com/science/article/pii/S0160738315000444>

Hartig T 1853 Ueber die Entwicklung des Jahrringes der Holzpflanzen *Bot Ztg* **11** 553–60

Hastenrath S 1963 Dendrochronologie in el Salvador *Meteorol. Rundschau* **16** 110–3

Hou Y, Zhou W, Cheng P, Xiong X, Du H, Niu Z, Yu X, Fu Y and Lu X 2020 ¹⁴C-AMS measurements in modern tree rings to trace local fossil fuel-derived CO₂ in the greater Xi'an area, China *Sci. Total Environ.* **715** 136669 Online:
<https://doi.org/10.1016/j.scitotenv.2020.136669>

- Hua Q, Turnbull J C, Santos G M, Rakowski A Z, Ancapichún S, De Pol-Holz R, Hammer S, Lehman S J, Levin I, Miller J B, Palmer J G and Turney C S M 2021 Atmospheric radiocarbon for the period 1950-2019 *Radiocarbon* **00** 1–23
- Hummel F 1946 The formation of growth rings in *Entandrophragma macrophyllum* A. Chev. and *Khaya grandifolia* C. D.C *Emp. For. Rev.* **25** 103–7 Online: <http://www.jstor.org/stable/42598941>
- Jeřkovský M, Povinec P P, Steier P, Šivo A, Richtáriková M and Golser R 2015 Retrospective study of ^{14}C concentration in the vicinity of NPP Jaslovské Bohunice using tree rings and the AMS technique *Nucl. Instruments Methods Phys. Res. Sect. B Beam Interact. with Mater. Atoms* **361** 129–32
- Kaennel M and Schweingruber F H 1995 *Multilingual glossary of dendrochronology* (Swiss Federal Institute for Forest, Snow and Landscape Research, WSL/FNP, Paul Haupt Publisher, Berne.)
- Karmakar D, Deb K and Padhy P K 2021 Ecophysiological responses of tree species due to air pollution for biomonitoring of environmental health in urban area *Urban Clim.* **35** 100741 Online: <https://doi.org/10.1016/j.uclim.2020.100741>
- Kontuľ I, Jeřkovský M, Kaizer J, Šivo A, Richtáriková M, Povinec P P, Čech P, Steier P and Golser R 2017 Radiocarbon concentration in tree-ring samples collected in the south-west Slovakia (1974–2013) *Appl. Radiat. Isot.* **126** 58–60
- Krepkowski J, Bräuning A, Gebrekirstos A and Strobl S 2011 Cambial growth dynamics and climatic control of different tree life forms in tropical mountain forest in Ethiopia *Trees* **25** 59–70 Online: <http://link.springer.com/10.1007/s00468-010-0460-7>
- Kutschera W 2019 The Half-Life of ^{14}C —Why Is It So Long? *Radiocarbon* **61** 1135–42
- Lee J 1979 The Impact of Oil Price Shocks on Oil Demand Growth *The 1979 “Oil Shock”: Legacy, Lessons, and Lasting Reverberations* pp 13–7
- Legendre P and Legendre L 2012 *Numerical Ecology* vol 24 (Amsterdam, Netherlands: Elsevier)

-
- Levin I 1987 Atmospheric CO₂ in continental Europe—an alternative approach to clean air CO₂ data *Tellus B* **39 B** 21–8
- Levin I, Kromer B, Schmidt M and Sartorius H 2003 A novel approach for independent budgeting of fossil fuel CO₂ over Europe by ¹⁴CO₂ observations *Geophys. Res. Lett.* **30** 1–5
- Levin I, Schuchard J, Kromer B and Munnich K O 1989 The continental European Suess effect *Radiocarbon* **31** 431–40
- Loader N J, Mccarroll D, Miles D, Young G H F, Davies D and Ramsey C B 2019 Tree ring dating using oxygen isotopes: a master chronology for central England *J. Quat. Sci.* **34** 475–90 Online: <http://dx.doi.org/10.1002/jqs.3115>
- Machado A, García N, García C, Acosta L and Córdova A 2008 Contaminación por metales (Pb , Zn , Ni y Cr) en aire, sedimentos viales y suelo en una zona de alto tráfico vehicular *Rev. Int. Contami. Ambient* **24** 171–82
- Madejo P, Maran T and Murillo J 2006 Biomonitoring of trace elements in the leaves and fruits of wild olive and holm oak trees *Sci. Total Environ.* **355** 187–203
- Miller J B, Lehman S J, Verhulst K R, Miller C E, Duren R M, Yadav V, Newman S and Sloop C D 2020 Large and seasonally varying biospheric CO₂ fluxes in the Los Angeles megacity revealed by atmospheric radiocarbon *Proc. Natl. Acad. Sci. U. S. A.* **117** 26681–7
- Miranda-Áviles R, Puy-Alquiza M J and Martínez-Reyes J J 2009 Potencial del Uso del Fresno (*Fraxinus udhei*) en Estudios Dendrocronológicos. *Concienc. Tecnológica* **38** 24–9
- Molina D A 2013 *La ciudad, sus árboles y los cuerpos: el proceso de modernización y la transformación del paisaje en Medellín (1890-1950)* (Universidad Nacional de Colombia) Online: <http://www.bdigital.unal.edu.co/45331/>
- Norrgård S and Helama S 2021 Dendroclimatic investigations and cross-dating in the 1700s : the tree-ring investigations of Johan Leche (1704–1764) in southwestern Finland *Can. J. For. Res.* **51** 267–73

-
- Palstra S W L, Karstens U, Streurman H J and Meijer H A J 2008 Wine ethanol ^{14}C as a tracer for fossil fuel CO_2 emissions in Europe: Measurements and model comparison *J. Geophys. Res. Atmos.* **113**
- Parmar T K, Rawtani D and Agrawal Y K 2016 Bioindicators: the natural indicator of environmental pollution *Front. Life Sci.* **9** 110–8 Online: <https://doi.org/10.1080/21553769.2016.1162753>
- Pataki D E, Randerson J T, Wang W, Herzenach M and Grulke N E 2010 The carbon isotope composition of plants and soils as biomarkers of pollution *Isoscapes: Understanding movement, pattern, and process on Earth through isotope mapping* ed Jason B West (Springer) pp 407–23
- Pazdur A, Nakamura T, Pawełczyk S, Pawlyta J, Piotrowska N, Rakowski A, Sensuła B and Szczepanek M 2007 Carbon isotopes in tree rings: climate and the suess effect interferences in the last 400 years *Radiocarbon* **49** 775–88
- Perilla-Henao L M, Dickinson M and Franco-Lara L 2012 First Report of ‘ Candidatus Phytoplasma asteris’ Affecting Woody Hosts (*Fraxinus uhdei*, *Populus nigra*, *Pittosporum undulatum* , and *Croton* spp.) in Colombia *Plant Dis.* **96** 1372–1372
- Pinheiro J, Bates D M, DebRoy S, Sarkar D, HeiSterkamp S, Van Willigen B, Ranke J and R Core Team 2021 Linear and Nonlinear Mixed Effects Models 1–338
- Pinheiro J C and Bates D M 2000 *Mixed-Effects Models in S and S-PLUS* ed Springer
- Piotrowska N, Pazdur A, Pawełczyk S, Rakowski A, Sensuła B and Tudyka K 2019 Human activity recorded in carbon isotopic composition of atmospheric CO_2 in Gliwice Urban Area and surroundings (Southern Poland) in the Years 2011–2013 *Radiocarbon* 1–16
- Prodan M 1968 *Forest Biometrics* (London, Uk: Pergamon Press)
- Quarta G, Rizzo G A, D’Elia M and Calcagnile L 2007 Spatial and temporal reconstruction of the dispersion of anthropogenic fossil CO_2 by ^{14}C AMS measurements of plant material *Nucl. Instruments Methods Phys. Res. Sect. B Beam Interact. with Mater. Atoms* **259** 421–5
- R Core Team 2020 R: A language and environment for statistical computing

-
- Rakowski A, Kuc T, Nakamura T and Pazdur A 2004a Radiocarbon concentration in the atmosphere and modern tree rings in the Kraków Area, Southern Poland *Radiocarbon* **46** 911–6
- Rakowski A, Nakamura T and Pazdur A 2004b Changes in radiocarbon concentration in modern wood from Nagoya, central Japan *Nucl. Instruments Methods Phys. Res. Sect. B Beam Interact. with Mater. Atoms* **223–224** 507–10
- Rakowski A, Nakamura T and Pazdur A 2008a Variations of anthropogenic CO₂ in urban area deduced by radiocarbon concentration in modern tree rings *J. Environ. Radioact.* **99** 1558–65
- Rakowski A, Nakamura T and Pazdur A 2008b Variations of anthropogenic CO₂ in urban area deduced by radiocarbon concentration in modern tree rings *J. Environ. Radioact.* **99** 1558–65
- Rakowski A, Nakamura T, Pazdur A and Meadows J 2013a Radiocarbon concentration in annual tree rings from the Salamanca Region, Western Spain *Radiocarbon* **55** 1533–40
- Rakowski A Z, Nakamura T, Pazdur A and Meadows J 2013b Radiocarbon concentration in annual tree rings from the Salamanca Region, Western Spain *Radiocarbon* **55** 1533–40
- Rakowski A Z, Pawelczyk S and Pazdur A 2001 Changes of ¹⁴C concentration in modern trees from upper Silesia region, Poland *Radiocarbon* **43** 679–89
- Romberger J A and Mikola P 1964 *International review of forestry research* (New York: Academic Pres) Online:
<http://www.sciencedirect.com/science/article/pii/S0160738315000444>
- Rozendaal D and Zuidema P A 2011 Dendroecology in the tropics : a review *Trees* **25** 3–16
- Santos G M, Granato-Souza D, Barbosa A C, Oelkers R and Andreu-Hayles L 2020 Radiocarbon analysis confirms annual periodicity in *Cedrela odorata* tree rings from the equatorial Amazon *Quat. Geochronol.* **58** 101079 Online:
<https://doi.org/10.1016/j.quageo.2020.101079>

-
- Sarton G 1954 When was tree-rings analysis discovered? *Isis* **45** 383–4
- Sawidis T, Breuste J, Mitrovic M, Pavlovic P and Tsigaridas K 2011 Trees as bioindicator of heavy metal pollution in three European cities *Environ. Pollut. J.* **159** 3560–70
- Scerbo R, Possenti L, Lampugnani L, Ristori T and Barale R 1999 Lichen (*Xanthoria parietina*) biomonitoring of trace element contamination and air quality assessment in Livorno Province (Tuscany, Italy) *Sci. Total Environ.* **241** 91–106
- Schneider C A, Rasband W S and Eliceiri K W 2012 NIH Image to ImageJ: 25 years of image analysis *Nat. Methods* **9** 671
- Schöngart J, Bräuning A, Campos A C M, Lisi C S and Morales J 2017 Dendroecological studies in the neotropics: history, status and future challenges *Dendroecology* vol 231 (Springer International Publishing) pp 35–73
- Semeraro T, Luvisi A, De Bellis L, Aretano R, Sacchelli S, Chirici G, Marchetti M and Coccozza C 2020 Dendrochemistry: Ecosystem Services Perspectives for Urban Biomonitoring *Front. Environ. Sci.* **8** 1–9
- Sensuła B, Michczyński A, Piotrowska N and Wilczyński S 2018 Anthropogenic CO₂ emission records in Scots Pine growing in the most industrialized region of Poland from 1975 to 2014 *Radiocarbon* **60** 1041–53
- Sensuła B and Pazdur A 2013 Stable carbon isotopes of glucose received from pine tree-rings as bioindicators of local industrial emission of CO₂ in Niepołomice Forest (1950–2000) *Isotopes Environ. Health Stud.* **49** 532–41
- Shestakova T A and Martínez-Sancho E 2021 Stories hidden in tree rings: A review on the application of stable carbon isotopes to dendrosciences *Dendrochronologia* **65**
- Speer J H 2010 *Fundamentals of tree-ring research* (University of Arizona Press)
- Spokas K, Graff C, Morcet M and Aran C 2003 Implications of the spatial variability of landfill emission rates on geospatial analyses *Waste Manag.* **23** 599–607
- Steinhof A, Altenburg M and Machts H 2017 Sample preparation at the Jena ¹⁴C laboratory *Radiocarbon* **59** 815–30

-
- Studhalter R 1956 Early History of Crossdating *Tree-Ring Bull.* 31–5
- Suess H E 1955 Radiocarbon concentration in modern wood *Science (80-)*. **122** 415–7
- Tans P and Kirk T 2018 ESRL Global Monitoring Division *US Dep. Commer. Earth Syst. Res. Lab.* 1 Online:
https://www.esrl.noaa.gov/gmd/dv/data/index.php?category=Greenhouse%2BGases¶meter_name=Carbon%2BDioxide
- Terekhina N V. and Ufimtseva M D 2020 Leaves of trees and shrubs as bioindicators of air pollution by particulate matter in Saint Petersburg *Geogr. Environ. Sustain.* **13** 224–32
- Toro M, Molina E, Garcia P, Quiceno D, Londoño A and Acevedo L 2013 *Inventario de emisiones atmosféricas del valle de Aburrá, año base 2011* (Medellín, Colombia: Universidad Pontificia Bolivariana - Área Metropolitana del valle de Aburrá)
- Toro M, Molina E, Medina J C, Gil L C, Gonzalez M I, Gómez P, Arcos Ó, Arbelaez J, Moncada S and Ruiz S 2018 *Actualización inventario de emisiones atmosféricas del valle de Aburrá- Año 2016* (Medellín, Colombia: Universidad Pontificia Bolivariana - Área Metropolitana del valle de Aburrá)
- Toro M, Molina E, Quiceno D, Frank O, Acevedo L, Arcos Ó, Orrego A and Arteaga D 2015 *Inventario de misiones atmosféricas del valle de Aburrá, año base 2013* (Medellín, Colombia: Universidad Pontificia Bolivariana - Área Metropolitana del valle de Aburrá)
- Toro M, Molina E, Roldan C, Gonzalez M I, Jaramillo L, Arcos Ó and Orrego A 2017 *Inventario de atmosféricas del valle de Aburrá, actualización 2015* (Medellín, Colombia: Universidad Pontificia Bolivariana - Área Metropolitana del valle de Aburrá)
- Trumbore S, Czimczik C I, Sierra C A, Muhr J and Xu X 2015 Non-structural carbon dynamics and allocation relate to growth rate and leaf habit in California oaks *Tree Physiol.* **35** 1206–22
- Turnbull J C, Keller E D, Baisden T, Brailsford G, Bromley T, Norris M and Zondervan A 2014 Atmospheric measurement of point source fossil CO₂ emissions *Atmos. Chem. Phys.* **14**

5001–14

- Turnbull J G, Graven H and Krakauer N Y 2016 Radiocarbon in the atmosphere *Radiocarbon and climate change* ed E A G Schuur, E R M Druffel and S E Trumbore (Springer International Publishing Switzerland) pp 83–139
- Varga T, Orsovszki G, Major I, Veres M, Bujtás T, Végh G, Manga L, Jull A J T, Palcsu L and Molnár M 2020 Advanced atmospheric ^{14}C monitoring around the Paks Nuclear Power Plant, Hungary *J. Environ. Radioact.* **213**
- Villanueva Díaz J, Pérez Evangelista E R, Beramendi Orozco L E and Cerano Paredes J 2015 Crecimiento radial anual del fresno (*Fraxinus udhei* (Wenz.) Lingelsh.) en dos parques de la Comarca Lagunera *Rev. Mex. Ciencias For.* **6** 40–57
- Vogel F R, Hammer S, Steinhof A, Kromer B and Levin I 2010 Implication of weekly and diurnal ^{14}C calibration on hourly estimates of CO₂-based fossil fuel CO₂ at a moderately polluted site in southwestern Germany *Tellus, Ser. B Chem. Phys. Meteorol.* **62** 512–20
- Wang P, Zhou W, Niu Z, Xiong X, Wu S, Cheng P, Hou Y, Lu X and Du H 2021 Spatio-temporal variability of atmospheric CO₂ and its main causes: A case study in Xi'an city, China *Atmos. Res.* **249** 1–9 Online: <https://doi.org/10.1016/j.atmosres.2020.105346>
- Webb G E 1983 *Tree rings and telescopes. The scientific career of AE Douglass.* (Tucson: University of Arizona Press)
- Worbes M 1999 Annual growth rings, rainfall-dependent growth and long-term growth patterns of tropical trees from the Caparo Forest Reserve in Venezuela *J. Ecol.* **87** 391–403
- Worbes M 2002 One hundred years of tree-ring research in the tropics - A brief history and an outlook to future challenges *Dendrochronologia* **20** 217–31
- Xu S, Cook G T, Cresswell A J, Dunbar E, Freeman S P H T, Hastie H, Hou X, Jacobsson P, Naysmith P and Sanderson D C W 2015 Radiocarbon concentration in modern tree rings from Fukushima, Japan *J. Environ. Radioact.* **146** 67–72 Online: <http://dx.doi.org/10.1016/j.jenvrad.2015.04.004>
- Xu S, Cook G T, Cresswell A J, Dunbar E, Freeman S P H T, Hastie H, Hou X, Jacobsson P,

Naysmith P, Sanderson D C W, Tripney B G and Yamaguchi K 2016 ¹⁴C levels in the vicinity of the Fukushima Dai-ichi Nuclear Power Plant prior to the 2011 accident *J. Environ. Radioact.* **157** 90–6 Online: <http://dx.doi.org/10.1016/j.jenvrad.2016.03.013>

Zhao H, Niu Z, Zhou W, Wang S, Shugang F, Lu X and Du H 2021 Measurement report: Source apportionment of carbonaceous aerosol using dual-carbon isotopes (¹³C and ¹⁴C) and levoglucosan in three northern Chinese cities during 2018–2019 *Atmos. Chem. Phys.* **2** 1–55

Zhou W, Wu S, Huo W, Xiong X, Cheng P, Lu X and Niu Z 2014 Tracing fossil fuel CO₂ using δ ¹⁴C in Xi'an City, China *Atmos. Environ.* **94** 538–45 Online: <http://dx.doi.org/10.1016/j.atmosenv.2014.05.058>